# Ligand-Directed Active Tumor-Targeting Polymeric Nanoparticles for Cancer Chemotherapy

Yinan Zhong, Fenghua Meng, Chao Deng,* and Zhiyuan Zhong*

Biomedical Polymers Laboratory, and Jiangsu Key Laboratory of Advanced Functional Polymer Design and Application, College of Chemistry, Chemical Engineering and Materials Science, Soochow University, Suzhou, 215123, People's Republic of China

ABSTRACT: In recent years, polymeric nanoparticles have appeared as a most viable and versatile delivery system for targeted cancer therapy. Various in vivo studies have demonstrated that virus-sized stealth particles are able to circulate for a prolonged time and preferentially accumulate in the tumor site via the enhanced permeability and retention (EPR) effect (so-called "passive tumor-targeting"). The surface decoration of stealth nanoparticles by a specific tumor-homing

ligand, such as antibody, antibody fragment, peptide, aptamer, polysaccharide, saccharide, folic acid, and so on, might further lead to increased retention and accumulation of nanoparticles in the tumor vasculature as well as selective and efficient internalization by target tumor cells (termed as "active tumor-targeting"). Notably, these active targeting nanoparticulate drug formulations have shown improved, though to varying degrees, therapeutic performances in different tumor models as compared to their passive targeting counterparts. In addition to type of ligands, several other factors such as in vivo stability of nanoparticles, particle shape and size, and ligand density also play an important role in targeted cancer chemotherapy. In this review, concept and recent development of polymeric nanoparticles conjugated with specific targeting ligands, ranging from proteins (e.g., antibodies, antibody fragments, growth factors, and transferrin), peptides (e.g., cyclic RGD, octreotide, AP peptide, and tLyp-1 peptide), aptamers (e.g., A10 and AS1411), polysaccharides (e.g., hyaluronic acid), to small biomolecules (e.g., folic acid, galactose, bisphosphonates, and biotin), for active tumor-targeting drug delivery in vitro and in vivo are highlighted and discussed. With promise to maximize therapeutic efficacy while minimizing systemic side effects, ligand-mediated active tumor-targeting treatment modality has become an emerging and indispensable platform for safe and efficient cancer therapy.
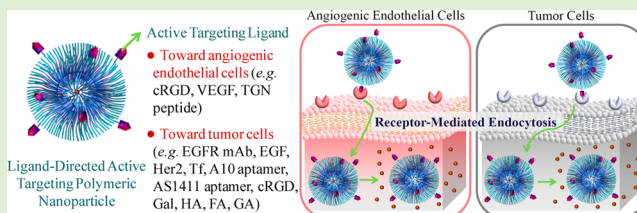
1. INTRODUCTION

In the past decades, drug research has evolved rapidly, which has led to the discovery of numerous potent chemotherapeutic agents. It should be noted, however, that, despite fast progress in drug innovation, little clinical impact on cancer chemotherapy has been made to date. This is likely because of the following reasons: (i) many potent drugs are sparingly water-soluble, which restrains them from the clinical applications; (ii) chemotherapeutic drugs are usually lack of specificity, which renders them while effective against cancer cells also highly toxic to healthy cells; (iii) most drugs suffer from an inappropriate biodistribution following i.v. administration, which results in low therapeutic efficacy as well as significant side effect; (iv) loads of drugs exhibit poor pharmacokinetics and bioavailability in vivo;[1] and (v) there is a modest understanding of tumor physiology[2] and role of immune system and cancer stem cells in cancer development.[3,4] The clinical success of chemotherapeutic drugs is dependent on selection of the right targets and drug combination as well as an appropriate delivery system that is able to deliver and release drug into the specific pathological site.[5,6] To this end, various forms of virus-sized drug vehicles ranging from liposomes, polymeric nanoparticles, mesoporous silica nanoparticles, to metallic nanoparticles have been developed and explored for controlled drug release applications.[7,8] In particular, polymeric nanoparticles have received the most attention in that (i) as

compared to liposomes, polymeric nanoparticles usually contain an intrinsically stealthy surface, possess enhanced in vivo stability, and, furthermore, can be designed and prepared with diverse polymer structures, molecular weights, compositions, and functions to meet the requirements of a particular drug and application; (ii) in contrast to silica and metallic nanoparticles, polymeric nanoparticles based on several synthetic and natural polymers such as biodegradable aliphatic polyesters, polypeptides, poly(ethylene glycol) (PEG), hyaluronic acid (HA), and dextran have demonstrated excellent safety and are approved by the authorities for various medical and pharmaceutical uses; and (iii) depending on purpose, polymeric nanoparticles can be tailor-made with distinct constructions ranging from macromolecular prodrugs, micelles, nanogels, to vesicles and varying particle sizes from 4 to 250 nm.[9,10] Interestingly, various in vivo studies have demonstrated that polymeric nanoparticles are able to circulate for a prolonged time and preferentially accumulate in the tumor site via the enhanced permeability and retention (EPR) effect (so-called "passive tumor-targeting").[11,12] In collaboration with medical doctors and pharmaceutical industries, a few polymer-based nanomedicines such as Genexol-PM,[13] NK 911,[14] NK 105,[15]

Scheme 1. Ligand-Directed Active Tumor-Targeting Polymeric Nanoparticles for Cancer Chemotherapy[a]
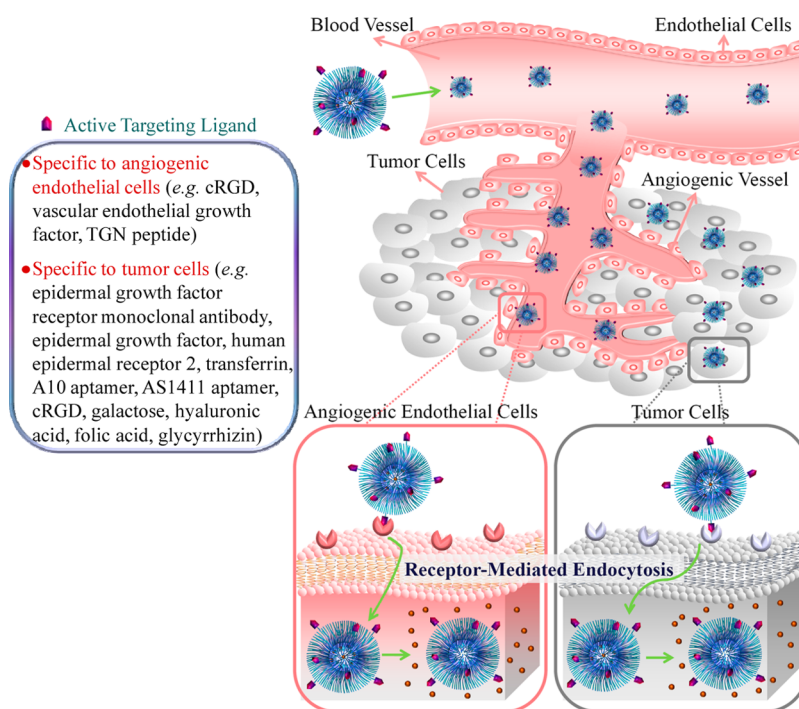
[a]There exist two active targeting strategies: (i) targeting to tumor cells and (ii) targeting to angiogenic endothelial cells.

and NC 6004[16] have been translated to the clinics or into different phases of clinical trials. This passive tumor-targeting treatment modality has demonstrated clear advantages of improved patient compliance, better drug tolerance, and decreased side effects over the current clinical approaches.

The therapeutic efficacy of passive tumor-targeting drug delivery systems is, nevertheless, far from optimal. One prime reason is the poor tumor cell uptake resulting from their stealth surface that is required for prolonged circulation.[17] The surface decoration of stealth nanoparticles by a specific tumor-homing ligand such as antibody, antibody fragment, peptide, aptamer, polysaccharide, saccharide, folic acid, and so on can largely increase retention and accumulation of nanoparticles in the tumor vasculature as well as selective and efficient internalization by target tumor cells, which is coined as "active tumor-targeting" (Scheme 1).[18] The in vitro and in vivo studies have shown that ligand-directed active targeting nanoparticulate drug formulations present improved, though to varying degrees, therapeutic performances as compared to their passive targeting counterparts.[19,20] It should be stressed that, besides targeting to tumor cells, tumor neovasculature represents the other interesting target for cancer chemotherapy as tumor angiogenesis is known of critical importance to the growth and metastasis of solid tumors (Scheme 1). The obliteration of tumor neovasculature will lead to shrinkage of established solid tumors via blocking blood supply (selective starvation of cancer).[20,21] In the past years, different types of targeting ligands such as cyclic RGD (cRGD), folic acid (FA), HA, human epidermal receptor 2 (Her2), galactose, glycyrrhizin, bisphosphonates, and (S,S-2-(3-(5-amino-1-carboxypentyl)-ureido)-pentanedioic acid) (ACUPA) have been employed for active tumor-targeting drug delivery. In addition to the type of ligands, the size, shape, and stability of nanoparticles, as well as the density and affinity of targeting ligand, also play an important role in targeted cancer chemotherapy.[22] It should be
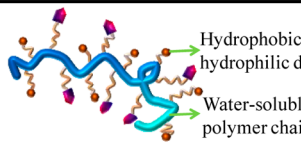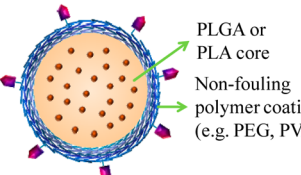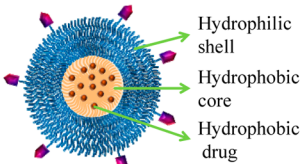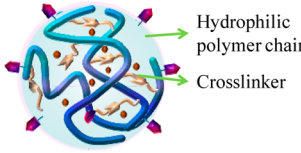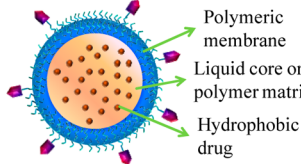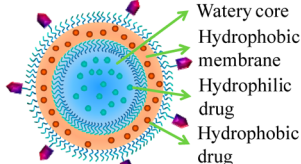
noted that development of ligand-directed active targeting nanomedicines remains at its infancy. Though a tremendous amount of preclinical studies on different nanoparticles and tumor models have been undertaken worldwide, few active targeting nanomedicines have advanced to the clinical trials.

With promise to maximize therapeutic efficacy as well as minimize systemic side effects, ligand-mediated active tumor-targeting modality has become an emerging and indispensable platform for safe and efficient cancer treatment. There are a few excellent reviews on targeting nanoparticles for cancer chemotherapy;[18,21,23,24] however, none of them focuses on active tumor-targeting polymeric nanoparticles. In this review, we introduce concept and recent development of active targeting polymeric nanoparticles for the treatment of different types of tumors. The pros and cons of different targeting systems are discussed. In the end, conclusions and future perspective on active targeting polymeric nanoparticles for cancer chemotherapy are presented.

2. LIGAND-DIRECTED ACTIVE TUMOR-TARGETING POLYMERIC NANOPARTICLES

Polymeric nanoparticles are a particularly versatile class of drug carrier systems.[25] In general, polymeric nanoparticles can be classified into macromolecular prodrugs, stealth nanoparticles, micelles, nanogels, nanocapsules, and vesicles (Table 1). The different types of nanoparticles have distinct shapes and physicochemical properties, which can be tailored to suit for delivery of diverse drugs. The conjugation of chemotherapeutic drugs to water-soluble polymer backbone via a cleavable linkage represents a simplest form of polymer-based nanoscale drug systems. They typically exist in unimers with average diameters of 4−15 nm.[26] These polymer−drug conjugates, while remaining inactive during circulation, could be activated at the targeted site by, for example, enzymes or acidic pH in the endo/lysosomal compartments.[27] It has to be realized, however,

Table 1. Structure and Characteristics of Various Ligand-Directed Active Tumor-Targeting Polymeric Nanoparticles

Nanosystem	Structure	Characteristics	Examples
Macromolecular prodrug	Hydrophobic or hydrophilic drug; Water-soluble polymer chain	(i) Size: 4 ~ 15 nm; (ii) Drugs are chemically conjugated to water-soluble polymer backbone; (iii) Inactive during circulation while activated at the site of action; (iv) Active targeting achieved by grafting ligand to the polymer	RGDfK-HPMA-DTX; Gal-HPMA-DOX
Stealth nanoparticle	PLGA or PLA core; Non-fouling polymer coating (e.g. PEG, PVA)	(i) Size: 100 ~ 350 nm; (ii) Able to carry hydrophobic and hydrophilic drugs; (iii) Targeting nanoparticles obtained by employing ligand-containing surfactant	Tf-PEG-HCPT; FA-PEG-DSPE/PEG-DSPE/DLPC
Micelle	Hydrophilic shell; Hydrophobic core; Hydrophobic drug	(i) Size: 10 ~ 100 nm; (ii) Core-shell architechture; (iii) Hydrophobic drug are loaded in the hydrophobic core; (iv) Targeting ligand introduced by attaching to the other terminal of the hydrophilic chain	EGF-PEG-PCL; A10-PEG-PLGA/PEG-PLGA; cRGD-PEG-P(Glu)
Nanogel	Hydrophilic polymer chain; Crosslinker	(i) Size: 20 ~ 250 nm; (ii) Hydrophilic polymer network; (iii) Drugs are loaded throughout the whole nanogel; (iv) Stable while fast responsive to environmental factors; (v) Active targeting obtained by conjugating ligand onto the outer surface	Gal-CS-*g*-PNIPAm
Nanocapsule	Polymeric membrane; Liquid core or polymer matrix; Hydrophobic drug	(i) Size: 100 ~ 500 nm; (ii) Consisting of an inner liquid core surrounded by a polymeric membrane; (iii) Hydrophobic drugs are loaded inside the capsule; (iv) Active targeting obtained by conjugating ligand onto the outer surface	FA-PEG/PEO-PPO-PEO
Polymersome	Watery core; Hydrophobic membrane; Hydrophilic drug; Hydrophobic drug	(i) Size: 10 nm ~ 10 μm; (ii) Polymeric vesicle containing a watery core; (iii) Able to carry both hydrophobic and hydrophilic drugs; (iv) Active targeting gained by installing ligand onto the other terminal of hydrophilic chains	Tf-PEG-PCL; Lf-PEG-PLA

that for nondegradable polymer carrier, polymer molecular weight can not exceed 40 kDa in order to be excreted from the body.[28]

Stealth nanoparticles refer to nanoscale particles based on, for example, poly(D,L-lactide) (PLA) and poly(D,L-lactide-*co*-glycolide) (PLGA) polymers that are coated with nonfouling water-soluble polymers such as PEG, dextran, and poly(acrylic acid) (PAA). It is important for nanoparticles to have a stealthy coating in order to achieve prolonged circulation times.[29] Employing preparation techniques such as nanoprecipitation, emulsification-solvent evaporation, and spray-drying, a variety of drugs, either hydrophilic (e.g., cisplatin, peptides, and proteins) or hydrophobic (e.g., paclitaxel (PTX) and doxorubicin (DOX)), can be encapsulated into stealth nanoparticles. The stealth nanoparticles are normally prepared with mean diameters of 100−350 nm.[30]

Polymeric micelles are typically self-assembled from amphiphilic block or graft copolymers. They have a characteristic core−shell structure and average diameters ranging from 10 to 100 nm. Micelles can significantly enhance water-solubility of lipophilic drugs and their bioavailability,[31] and have recently emerged as one of the most ideal systems for targeted delivery of sparingly water-soluble drugs such as PTX, docetaxel (DTX), and DOX.[32,33] However, one practical issue with polymeric micelles is that they tend to dissociate and release payloads upon extensive dilution and interaction with proteins and cells in the blood pool, which often lead to premature drug release following i.v. injection.[34]

Nanogels are nanosized hydrophilic polymer networks (20−250 nm) that are either physically or chemically cross-linked.[35] Nanogels possess several interesting properties such as good biocompatibility, excellent stability (in particular, for chemically cross-linked nanogels), and fast responsiveness to environmental factors, such as ionic strength, pH, and temperature.[36] Furthermore, nanogels can be chemically modified with various ligands for targeted drug delivery.[37] In order to achieve good drug loading and inhibit premature drug release, functional groups that show particular physical interactions with drugs are

usually introduced or drugs are chemically conjugated to nanogels.

Nanocapsules are nanovesicular systems containing a nontoxic polymeric membrane that encapsulates an inner liquid (aqueous or oily) core.[38] They can be prepared by different techniques such as layer-by-layer (LBL) assembly, emulsion–diffusion, nanoprecipitation, polymer-coating, and solvent-evaporation. The liquid core can be filled with a large amount of drugs, while the membrane can be engineered to achieve controlled drug release and targeted delivery. They are generally obtained with average sizes of 100–500 nm.[39]

Polymersomes are polymeric vesicles that contain a watery core and are prepared by self-assembly of amphiphilic block copolymers in aqueous conditions. The size of polymersomes can span from tens of nanometers to tens of micrometers.[40] It is interesting to note that polymersomes can not only be used to deliver hydrophobic drugs but also hydrophilic drugs such as peptides, proteins and siRNA. The membrane of polymersomes, owing to their higher molecular weights and existing chain entanglements, is in general thicker, stronger, and tougher than liposomes.[41]

Active tumor-targeting can be achieved by functionalizing the polymeric nanoparticles with a specific ligand such as FA, saccharides, peptides, aptamers, antibodies, and antibody fragments (Table 1).[42] For example, tumor-targeting prodrugs are usually prepared by grafting ligands to the polymer carrier backbones. Active tumor-targeting micelles and polymersomes are typically obtained by installing ligands onto the other terminal of hydrophilic chains of amphiphilic block copolymers. The stealth nanoparticles can be bestowed with active targeting property by employing functional surfactants containing a specific ligand. Active targeting nanogels and nanocapsules are usually obtained by conjugating ligands onto their outer surfaces by, for example, click and carbodiimide chemistry. It should be noted that installation of targeting ligands not only will facilitate specific tumor cell uptake but also may further enhance retention and accumulation of nanoparticles in the tumor vasculature, which would result in significantly improved therapeutic efficacy and reduced systemic toxicity.

The in vivo performance of targeted nanoparticles is associated with a number of parameters, including size, shape, and stability of nanoparticles as well as the nature, density and affinity of targeting ligand. In order to achieve prolonged circulation time and elevated tumor accumulation, nanoparticles are better having hydrodynamic sizes in a range of 20 to 200 nm, depending on type and states of tumors. However, small particle sizes are generally more desirable for tumor penetration. The shape of nanoparticles might have an impact on their in vivo biodistribution as well as cellular trafficking behaviors.[43,44] The stability of nanoparticles in blood circulation remains a critical hurdle for efficient tumor-targeting drug delivery. It is often found that a significant amount of drug would quickly leak out from the nanoparticles following i.v. administration. This premature drug release is one of the major causes for low drug accumulation in the tumor site. In the past several years, various strategies have been explored to enhance the in vivo stability of drug-loaded nanoparticles for better targetability.[45,46] It should be noted that tumor targetability is intimately dependent on type and position of ligands. Some ligands like antibodies are highly specific, while other ligands, such as cRGD and FA, are more ubiquitous and can target to different types of cells. To realize the targeting effect, ligands have to be fully exposed at the outer surface of nanoparticles.

The ligand density, however, should be optimized, depending on types of ligands and nanoparticles, to achieve high tumor accumulation and penetration as well as efficient and specific internalization by tumor cells.[47]

3. PROTEIN-DIRECTED ACTIVE TARGETING POLYMERIC NANOPARTICLES

In the past decades, various proteins such as antibodies, antibody fragments, growth factors, transferrin, and lactoferrin have been employed to achieve active tumor-targeting effect (Table 2). Among them, antibodies (Abs) stand for the most

Table 2. Protein-Directed Active Targeting Polymeric Nanoparticles for Cancer Treatment

construction	drug	target	ref
EGFR mAb-PLGA/PVA nanoparticles	rapamycin	breast cancer	49
ScFvEGFR-heparin-cisplatin nanoparticles	cisplatin	lung cancer	50
EGF-PEG-PCL micelles	ellipticine	breast cancer	51
bEGF-gelatin-cisplatin glutaraldehyde cross-linked nanoparticles	cisplatin	lung cancer	53
EGF-GemC18 nanoparticles	gemcitabine	breast cancer	54
P(TMCC-co-LA)-g-PEG-furan-Her2/P(TMCC-co-LA)-g-PEG-furan-doxorubicin nanoparticles	DOX	breast cancer	55
Her2-PEG-PLGA/PLGA nanoparticles	DTX	breast cancer	56
Her2-TPGS/PLA-TPGS nanoparticles	DTX	breast cancer	57
Her2-PEG-PLA nanoparticles	PTX	prostate cancer	58
HAb18 F(ab′)₂-PEG-PLGA-DOX micelles	DOX	liver cancer	59
HIF-1α Ab-PEO-b-PPO-b-PEO micelles	PTX	stomach cancer	60
Tf-HPAE-co-PLA/DPPE nanoparticles	PTX	cervical cancer	61
Tf-PEG-PHDCA noisomes	HCPT	mice sarcoma	62
Tf-PEG-HCPT stealth nanoparticles	HCPT-PEG	mice sarcoma	63
Tf-TPGS/PLA-TPGS nanoparticles	DTX	brain glioma	64
Tf-PEG-PCL polymersomes	DOX	brain glioma	65
Lf-PEG-PLA polymersomes	DOX	brain glioma	66

well-known and efficient targeting ligands. Abs possesses a high specificity and affinity to the corresponding antigens, with dissociation constants in the nanomolar range. Abs typically consists of two large heavy chains and two smaller light chains. In some cases, a targeting ligand can also be made of the variable region of the Abs, allowing a drastic reduction of total molecular weight as well as adverse immune reactions.[48] The monoclonal antibodies (mAbs) and their fragments have been most widely employed in the active targeting schemes and about 30 of them have been approved for clinical uses.[22] Two receptor tyrosine kinases, epidermal growth factor receptor (EGFR) and Her2, have been extensively investigated for cancer therapy.[21] EGFR is overexpressed in a variety of solid tumors such as nonsmall cell lung cancer, squamous cell carcinoma of the head and neck, as well as breast, ovarian, kidney, pancreatic, and prostate cancer.[24] EGFR-targeted
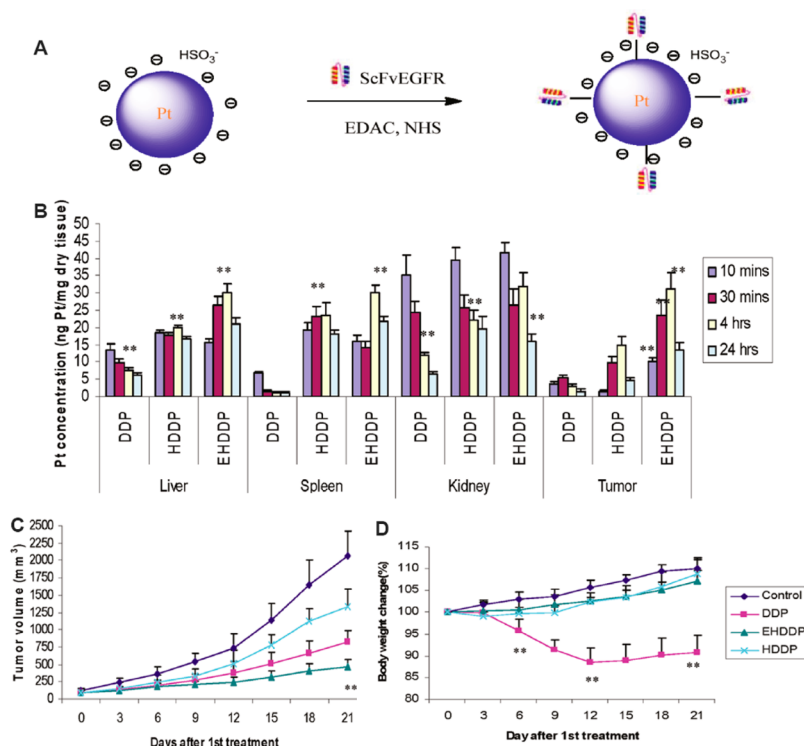
Figure 1. EGFR-decorated cisplatin-conjugated heparin-based nanoparticle (EHDDP) for targeted cisplatin delivery to lung tumor: (A) illustration on preparation of EHDDP; (B) biodistribution of Pt in nude mice bearing H292 tumors at different time points after i.v. injection of DDP, HDDP, and EHDDP; (C) tumor growth rate; and (D) body weight change (%) of H292 cell-bearing nude mice treated with DDP, HDDP, and EHDDP (2.5 mg Pt/kg, injection every 3 days, 5 injections, $n = 6$). The data are shown as mean $\pm$ SD ($*p < 0.05$, $**p < 0.01$). Reproduced from ref 50. Copyright 2011 American Chemical Society.

immuno-nanoparticles showed enhanced antitumor effects in vitro and in vivo. For example, the installation of EGFR mAb onto the surface of rapamycin-loaded PLGA/poly(vinyl alcohol) nanoparticles (EGFR mAb-PLGA/PVA) resulted in 17 times higher uptake by malignant breast cancer cells (MCF-7) than the corresponding nontargeting nanoparticles.[49] EGFR mAb-PLGA/PVA displayed superior antiproliferative activity toward MCF-7 cells with a half maximal inhibitory concentration (IC_{50}) of 26.11 ng/mL, which was significantly lower than for free rapamycin (268.9 ng/mL) and nontargeting counterparts (1.734 μg/mL). Wang et al. prepared an EGFR-targeted cisplatin-conjugated heparin-based nanoparticle (EHDDP) by functionalizing the nanoparticle surface with single chain variable fragment EGFR Ab (ScFvEGFR) via carbodiimide chemistry (Figure 1).[50] EHDDP exhibited 7.5-fold longer blood circulation time than free cisplatin, and 3- and 9-fold higher tumor accumulation than the nontargeted nanoparticle and free cisplatin, respectively. The in vivo studies in nonsmall lung cancer (H292)-bearing nude mice showed that EHDDP markedly suppressed tumor growth with little side effect. It is interesting to note that epidermal growth factor (EGF) can act as a targeting ligand as well as an apoptotic factor against EGFR overexpressing cancers. Allen et al. reported that EGF-conjugated PEG-poly(ε-caprolactone) (EGF-PEG-PCL) micelles, while being nonantiproliferative to cells expressing a low level of EGFR, were 13-fold more potent than free EGF against EGFR-overexpressing MDA-MB-468 cells (IC_{50} = ca. 0.076 vs 0.98 nM).[51] Notably, ellipticine-loaded EGF-PEG-PCL micelles demonstrated clearly a synergistic growth inhibitory effect toward MDA-MB-468 cells. The introduction of EGF molecular targeting, however,

imposed the "binding site barrier" effect, which halted the tumor penetration of EGF targeted PEG-PCL micelles with small size of 25 nm in vivo.[52] Lin et al. found that cisplatin-conjugated gelatin nanoparticles modified with biotinylated-EGF (GP-Pt-bEGF) showed a greater antitumor efficacy against human A549 adenocarcinoma xenografts in SCID mice by intratumoral injection than free cisplatin and nontargeting formulations (average relative tumor volume: ca. 31.82% vs 80.95% and 102.85%, respectively, following 17 days of treatment).[53] The treatment of mice with lung cancer via aerosol delivery showed that inhaled GP-Pt-bEGF could target and achieve high drug concentration in EGFR overexpressing cancerous lung. Cui et al. reported that both cellular uptake and cytotoxicity of recombinant murine EGF-conjugated 4-(N)-stearoyl gemcitabine nanoparticle (EGF-GemC18-NP) were correlated to the EGFR densities on the human breast adenocarcinoma cells.[54] The ex vivo imaging showed that EGF-GemC18-NPs had over 2-fold accumulation into EGFR overexpressing MDA-MB-468 tumors in mice as compared to ovalbumin conjugated GemC18-NPs (OVA-GemC18-NPs, nontargeting control). The growth of MDA-MB-468 tumors was significantly slower for mice treated with EGF-GemC18-NPs than with OVA-GemC18-NPs.

Her2 is overexpressed in a significant proportion of breast, gastric, and ovarian cancers. Her2 Abs like the humanized Her2 mAb (trastuzumab) have been developed for cancer treatment as well as targeted anticancer drug delivery.[67] Shoichet et al. obtained DOX-conjugated Her2-targeted immuno-nanoparticles (NP-aHer2-DOX) by coupling Her2 Ab and DOX to the furan groups on the surface of poly(2-methyl-2-carboxytri-methylene carbonate-co-D,L-lactide)-graft-poly(ethylene gly-

col)-furan (P(TMCC-*co*-LA)-*g*-PEG-furan) nanoparticles via Diels−Alder (DA) chemistry.[55] NP-aHer2-DOX exhibited enhanced cellular uptake and greater apoptotic activity as compared to nontargeting nanoparticles (IC$_{50}$ = 5.0 vs 10.0 μg/mL) in Her2 overexpressing SKBR-3 cells. Feng et al. prepared DTX-loaded PEG-PLGA/PLGA nanoparticles with varying herceptin surface densities by adjusting PLGA-PEG-NH$_2$/PLGA copolymer blend ratio during nanoprecipitation or herceptin to NH$_2$ on the nanoparticle surface feed molar ratio during postconjugation of antibody.[56] This DTX delivery system showed an obvious targeting effect to Her2 receptor overexpressed breast cancer cells (SK-BR-3) and the surface density of herceptin on the nanoparticles positively impacted on their in vitro performance. In a similar way, Her2-targeted nanoparticles with tailored surface densities of herceptin were developed based on PLA-D-α-tocopheryl poly(ethylene glycol) succinate (PLA-TPGS) and carboxyl group terminated TPGS (TPGS-COOH) copolymers for targeted delivery of DTX to Her2 receptor overexpressed breast cancer cells.[57] Benita et al. reported that paclitaxel palmitate (pcpl)-loaded trastuzumab-functionalized immuno-nanoparticles (pcpl immunoNPs) based on PEG-PLA showed 3 and 5 times higher uptake by prostate cancer cell line (PC-3 cells) following 3 h incubation than pcpl NPs (nontargeting control) and free pcpl, respectively.[58] The pharmacokinetics and biodistribution studies revealed that though pcpl immunoNPs and pcpl NPs had similar residence time and area under curve (AUC) following i.v. injection, significantly less accumulation in the liver and spleen was observed for pcpl immunoNPs. The pharmacological evaluation showed that pcpl immunoNPs inhibited the prostate tumor growth much more efficiently than the nontargeting pcpl NPs and free pcpl.

In addition to anti-EGFR antibodies, a couple of other receptor-specific antibodies have been employed for targeted cancer chemotherapy. For example, DOX-PLGA-PEG micelles were decorated with bivalent fragment HAb18 F(ab′)$_2$, which could bind to human hepatoma cells (Huh7 and HepG2 cells) with a high affinity.[59] A total of 2 h following i.v. injection into the nude mice bearing HepG2 xenograft, the targeted micelles were preferentially accumulated in the tumors, while the nontargeted micelles obviously accumulated in the liver and spleen. As a result, the targeted system exhibited the highest tumor inhibition rate compared to the nontargeted counterpart and free DOX (63.9% vs 50.2% and 39.8%, respectively). Human hypoxia inducible factor-1α (HIF-1α) Ab, which can target to cancer cells overexpressing HIF-1α (e.g., stomach cancer MGC-803 cells), was conjugated to the carboxyl group on the surface of PTX-loaded poly(ethylene oxide)-*block*-poly(propylene oxide)-*block*-poly(ethylene oxide) (PEO-*b*-PPO-*b*-PEO) micelles (anti-HIF-1α-NMs-PTX).[60] The results showed that anti-HIF-1α-NMs-PTX was taken up much more efficiently by MGC-803 cells than by HDF fibroblast cells (low expression of HIF-1α). These immuno-micelles could specifically target and selectively kill MGC-803 cells and markedly decrease the toxic side effects of PTX. It is evident that antibodies and antibody fragments are proper ligands to achieve active tumor targeting. However, they suffer drawbacks of low stability, large size, high cost, and potential immunogenicity. It should further be noted that both Abs and Ab fragments might be challenged with decreased affinity toward receptors as a result of chemical conjugation, interaction with circulating free antigen, and insufficient tumor penetration.[68]

Transferrin (Tf) is a serum nonheme iron-binding glycoprotein that helps transportation of iron to proliferating cells. Upon binding to the transferrin receptor on the cell surface, the transferrin is endocytosed into acidic compartments where the iron dissociates. The transferrin receptor plays a vital role in the regulation of cell growth and is overexpressed in malignant cells (up to 100-fold higher than that in normal cells).[69] Wu et al. reported that PTX-loaded Tf-functionalized nanoparticles based on hyperbranched poly((amine-ester)-*co*-LA)/1,2-dipalmitoyl-*sn*-glycero-3-phosphoethanolamine copolymer (HPAE-*co*-PLA/DPPE) exhibited 2-fold lower IC$_{50}$ in Tf receptor overexpressed human cervical carcinoma cells (HeLa cells) than free PTX and nontargeting counterparts.[61] Pei et al. prepared active targeting niosome (Tf-PEG-NS) by conjugating Tf to poly(ethylene glycol) cyanoacrylate-*co*-hexadecyl cyanoacrylate (PEG-PHDCA) modified niosomes for delivery of hydroxycamptothecin (HCPT).[62] The in vitro studies showed that compared with free HCPT, nonstealth noisome (n-NS) and PEG-NS formulations, HCPT-loaded Tf-PEG-NS had the greatest intracellular uptake and the highest cytotoxicity in all three carcinoma cell lines (KB, K562, and S180 cells). The in vivo studies in S180 tumor-bearing mice revealed that HCPT-loaded Tf-PEG-NS exhibited the greatest tumor inhibition rate of 71% at a low dose of 1 mg/kg, which was 1.55−2.40-fold higher than those of free HCPT and nontargeting counterparts. In a following study, Tf-modified stealth nanoparticle (Tf-PEG-NP) loaded with PEGylated HCPT was developed.[63] The pharmacokinetic and biodistribution studies displayed that PEG-HCPT loaded Tf-PEG-NP had 8.94-fold longer retention time in blood, 9.03-fold higher tumor accumulation, and 1.85-fold higher tumor inhibition rate in S180 tumor-bearing mice as compared to PEG-HCPT. Interestingly, transferrin receptor (TfR) is also overexpressed in the endothelial cells of the blood−brain barrier (BBB). Feng et al. developed Tf-conjugated PLA-TPGS nanoparticles for enhanced drug delivery to brain glioma cells (C6).[64] IC$_{50}$ data showed that DTX-loaded Tf-conjugated PLA-TPGS NPs was 23.4, 16.9, and 22.9% more efficient than formulations of PLGA NPs, PLA-TPGS NPs, and Taxotere, respectively, after 24 h treatment in C6 cells. The preliminary ex vivo biodistribution investigation demonstrated that Tf-conjugated PLA-TPGS NPs were able to deliver imaging/therapeutic agents across the BBB. Jiang et al. designed DOX-loaded Tf-conjugated biodegradable PEG-PCL polymersomes (Tf-PO-DOX) to increase both the BBB permeability and intracellular drug delivery to C6 cells.[65] The results showed that compared with PO-DOX and free DOX, Tf-PO-DOX revealed the greatest intracellular delivery and the strongest cytotoxicity in C6 cells. The in vivo studies in glioma-bearing rats showed that Tf-PO-DOX resulted in a significant reduction of tumor volume, which was 2.6-, 5.3-, and 5.7-fold smaller than those treated with PO-DOX, free DOX, and saline control group at 14 d and, accordingly, a significant increase of median survival time.

Lactoferrin (Lf) is another iron-binding protein which can bind to low-density lipoprotein receptor (LRP) overexpressed in the glioma cells. Lf has been investigated as a specific targeting molecule to promote the delivery of anticancer drugs to the brain.[70] Jiang et al. reported that Lf-installed PEG-PLA polymersome (Lf-PO) loaded with DOX and multidrug resistance (MDR) inhibitor tetrandrine (Tet) displayed 2-fold higher accumulation at the tumor site and 4.5 times better

inhibition of tumor growth in C6 glioma-bearing rats than the nontargeting counterparts (PO-DOX/Tet).[66]

4. APTAMER-DIRECTED ACTIVE TARGETING POLYMERIC NANOPARTICLES

Aptamers are single-stranded DNA or RNA that can bind to various molecular ligands with high specificity and affinity.[71] In contrast to antibodies, aptamers have a small size, are easy to synthesize, show high in vivo stability, and possess good solubility in different solvents.[72] In recent years, aptamers have appeared as a valuable alternative to antibodies and antibody fragments for targeted delivery of chemotherapeutic drugs (Table 3). A10 aptamer that specifically recognizes the

Table 3. Aptamer-Directed Active Targeting Polymeric Nanoparticles for Cancer Treatment

construction	drug	target	ref
A10-PEG-PLGA/PEG-PLGA micelles	DTX	prostate cancer	73
A10-PEG-PLGA/PEG-PLGA micelles	cisplatin + DTX	prostate cancer	74
A10-PEG-PLGA-H40 micelles	DOX	prostate cancer	75
GMT8-PEG-PCL/MPEG-PCL nanoparticles	DTX	brain glioma	76
AS1411-PEG-PLGA/HOOC-PEG-PLGA nanoparticles	PTX	brain glioma	77
AS1411-PEG-PCL/MPEG-PCL nanoparticles	DTX	brain glioma	78

extracellular domain of the prostate-specific membrane antigen (PSMA) abundantly expressed on the surface of the prostate cancer cells has been widely used for active targeting drug delivery to prostate cancer. Langer et al. prepared a series of targeted NPs with increasing Apt densities from PEG-*b*-PLGA and A10 aptamer (Apt)-decorated PEG-*b*-PLGA (PLGA-*b*-PEG-*b*-Apt), and investigated the influence of Apt density on biodistribution and targetability (Figure 2).[73] The results showed that increasing PLGA-*b*-PEG-*b*-Apt in the formulation to 5% led to 5-fold increase in NP uptake by PSMA overexpressing prostate cancer (LNCaP) cells. Further increase in PLGA-*b*-PEG-*b*-Apt proportion resulted in a modest increase in NP uptake. The presence of high Apt surface density, however, also led to enhanced NP accumulation in the liver and spleen, which is likely due to the fact that Apt has compromised the antifouling properties of PEG in NPs. In a following work, A10 aptamer-decorated nanoparticles were prepared with a diameter of ~100 nm from PLA derivative with platinum(IV) prodrug and carboxyl-terminated PEG–PLGA in microfluidic channels, followed by conjugation with A10 aptamer, for codelivery of cisplatin and DTX to prostate cancer cells.[74] In vitro toxicities in LNCaP cells revealed superiority of A10-decorated dual-drug formulations over single drug formulations and nontargeted counterparts. Gong et al. reported that DOX-loaded A10 aptamer-conjugated unimolecular micelles based on hyperbranched polyester (H40) core and PEG-PLA arms displayed pH-sensitive and controlled drug release behavior.[75] The aptamer-conjugated micelles exhibited a much higher cellular uptake and significantly higher cytotoxicity in PSMA positive CWR22Rn1 prostate carcinoma cells. The ex vivo imaging showed that DOX-loaded aptamer-conjugated targeted micelles exhibited a much higher DOX level in the CWR22Rn1 tumors in nude mice than nontargeted micelles and free DOX. GMT8 aptamer, a short DNA sequence that could specifically bind with glioblastoma U87 cells, was used to functionalize DTX-loaded PEG-PCL nanoparticles.[76] The results showed that DTX-loaded ApNP significantly induced cell apoptosis and inhibited tumor spheroid growth. The in vivo imaging demonstrated that in an orthotropic brain glioblastoma model, ApNP could target to glioblastoma resulting in 2-fold higher tumor accumulation than nontargeted controls. AS1411, a DNA aptamer specifically binding to nucleolin that is highly
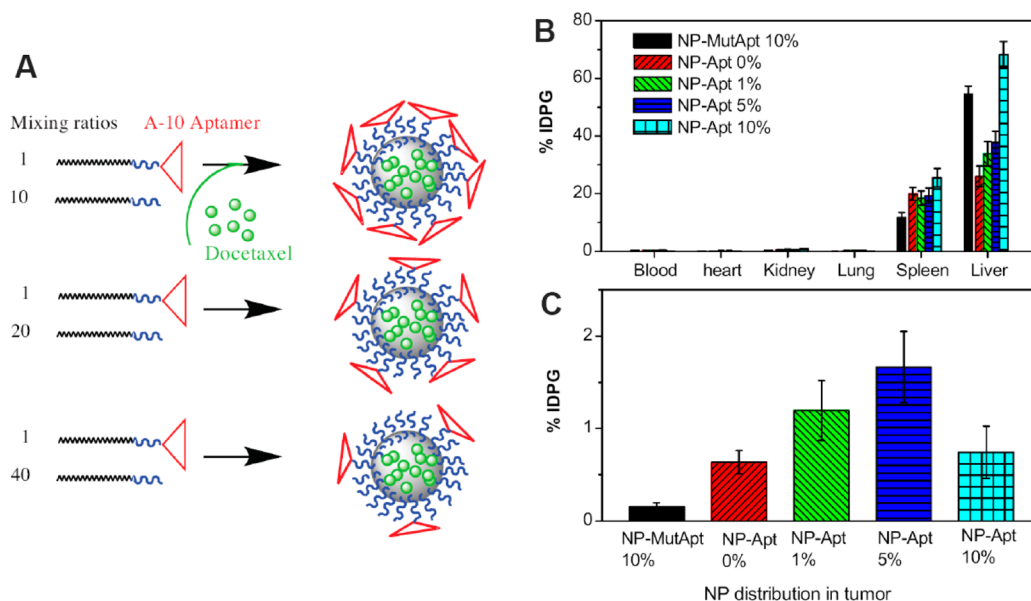

Figure 2. A10 aptamer-functionalized PEG-*b*-PLGA nanoparticles for targeted drug delivery to prostate tumor. (A) Aptamer-functionalized PEG-*b*-PLGA nanoparticles (NP-Apt) with different Apt surface densities; and (B, C) biodistribution in LNCaP tumor-bearing mice following retro-orbital injection of NP-Apt with different Apt surface densities (*n* = 5). The control groups were NPs without aptamers (NP-Apt 0%; red) and NPs with scrambled nonfunctional Apt (NP-MutApt 10%). The data are shown as mean ± SD. Reproduced with permission from ref 73. Copyright 2008 The National Academy of Science of the U.S.A.

expressed in the plasma membrane of both cancer cells such as glioblastoma (C6 cells) and endothelial cells in angiogenic blood vessels, has been widely used for glioma-targeted drug delivery. For example, Chen et al. conjugated AS1411 to the surface of PEG-PLGA NPs via the carbodiimide reaction.[77] PTX-loaded targeted nanoparticle (AS1411-PTX-NP) showed a prolonged circulation time in rats (half-life of 4.16 h), a high tumor inhibition of 81.68% in mice bearing C6 glioma xenograft, and prolonged animal survival on rats bearing intracranial C6 gliomas when compared with PTX-NP and Taxol treatments. Zhang et al. found that AS1411 could be combined with other ligand such as phage-displayed TGN peptide to enhance glioma penetration of DTX-loaded PEG-PCL nanoparticles and improve antiglioma effects.[78] This combined targeting system could target both endothelial cells and tumor cells and, moreover, could penetrate the endothelial cells monolayer and tumor spheroid to reach the center of the tumor mass, resulting in 3.91-fold higher glioma accumulation in BALB/c nude mice bearing C6 orthotopic glioma in vivo than the nontargeted group.

Though aptamers have many advantages over antibodies, they are still challenged by several limitations such as changeable specificity aroused from inconstant formation of aptamers' secondary or tertiary conformation both in vitro and in vivo, chemical instability in blood circulation induced from degradation by the serum nuclease, and relatively high manufacturing cost.[79]

5. PEPTIDE-DIRECTED ACTIVE TARGETING POLYMERIC NANOPARTICLES

In comparison to proteins, peptides have several advantages such as low production cost, good stability, capable of large-scale synthesis, easy manipulation, and reduced immune reaction. Moreover, conjugation of peptides can be precisely controlled by engineering a specific reactive group. The physicochemical properties of nanoparticles would hardly be altered by conjugating peptides owing to their relatively small sizes.[80] Table 4 summarizes peptide-directed active targeting polymeric nanoparticles for cancer treatment. cRGD has a high affinity with the $\alpha_v\beta_3$ integrin receptors overexpressed on both the endothelial cells and many types of solid tumors, which render them of particular interests as targets for anticancer drug delivery.[81] Gao et al. successfully conjugated cRGDfK to DOX-loaded PEG-PCL micelles by using a postmodification method.[82] The attachment of cRGDfK ligand greatly enhanced internalization of the micelles in $\alpha_v\beta_3$ integrin overexpressed SLK tumor endothelial cells, in which 30-fold enhancement of cellular uptake was observed for 76% cRGDfK-functionalized DOX-loaded micelles. In a following study, multifunctional micelles with cRGDfK on the micelle surface while DOX and a cluster of superparamagnetic iron oxide (SPIO) nanoparticles loaded inside the micelle core were developed for cancer-targeted and MRI-ultrasensitive drug delivery.[83] The rapid and efficient $\alpha_v\beta_3$-mediated endocytosis led to significant darkening of MR images from cRGDfK-encoded micelles compared to nontargeting micelles and a remarkable reduction of cell growth from 42.8 ± 2.0% for nontargeting micelles to 7.0 ± 1.4% for micelles containing 16% cRGDfK after 4 h incubation. Lippard et al. reported that cisplatin prodrug-encapsulated cRGD-functionalized PEG-PLGA nanoparticles displayed relatively high tumor growth inhibition of about 60%, with little change of body weight in an orthotopic human breast cancer (MCF7MFP1 with low level of $\alpha_v\beta_3$ integrin expression)

Table 4. Peptide-Directed Active Targeting Polymeric Nanoparticles for Cancer Treatment

construction	drug	target	ref
cRGD-PEG-PCL micelles	DOX	tumor endothelium	82,83
cRGD-PEG-PLGA nanoparticles	cisplatin	angiogenic endothelium	84
cRGD-PEG-PLA micelles	PTX	brain glioma	85
cRGDyk-PEG-PTMC micelles	PTX	brain glioma	86
cRGD-PEG-P(Glu) micelles	DACHPt	brain glioma	87
cRGD-PEO-PCL/ cRGD-PEO-PBCL micelles	PTX	breast cancer	88
P160-PEO-PCL/P160-PEO-PBCL micelles	PTX	breast cancer	88
cRGD-PLL-PLGA-MPEG nanoparticles	mitoxantrone	breast cancer	89
cRGD-PEO-PCL micelles	DOX	bladder cancer	90
(PGA)-PTX-E-cRGDfK₂ nanoparticles	PTX	angiogenic endothelium, glioblastoma, murine breast cancer	91
RGDfK-HPMA-DTX prodrugs	DTX	prostate cancer	92
iRGD-PVP-PCL micelles	PTX	murine hepatic cancer	93
Oct-PEG-PCL micelles	PTX	breast cancer	94
AP-PEG-PLA/MPEG-PAE micelles	DOX	breast cancer	95
tLyp-1-PEG-PLA nanoparticles	PTX	brain glioma	96

xenograft model in vivo.[84] The tumor inhibition was mainly due to effective inhibition of endothelial cells of the angiogenic vasculature. cRGD is most frequently served as the targeting ligand for the treatment of malignant gliomas in the central nervous system due to the high expression of $\alpha_v\beta_3$ integrin on the surface of glioblastoma cancer cells. For example, Lu et al. reported that PTX-loaded cRGDyK-PEG-PLA micelles (cRGDyK-PEG-PLA-PTX) demonstrated 2.5-fold enhanced antiglioblastoma cell cytotoxic efficacy.[85] The biodistribution studies showed that in U87MG glioblastoma-bearing nude mice model, cRGDyK-PEG-PLA micelles accumulated in the subcutaneous and intracranial tumor tissue. Compared with nontargeting PEG-PLA-PTX micelles and Taxol, cRGDyK-PEG-PLA-PTX exhibited the strongest tumor growth inhibition and the longest median survival time. Jiang et al. reported that PTX-loaded cRGDyK-functionalized PEG-b-poly(trimethylene carbonate) (PEG-PTMC) nanoparticles (cRGDyK-MNP/PTX) showed enhanced cellular uptake and more potent in vitro cytotoxicity toward U87MG cells than MNP/PTX and Taxol (IC$_{50}$: 0.022 μg/mL vs 0.051 and 0.058 μg/mL, respectively).[86] In vivo multispectral fluorescent imaging indicated that c(RGDyK)-MNP/PTX could substantially home to integrin-rich U87MG tumor and decrease nonspecific uptake by the reticuloendothelial systems (RES). Kataoka et al. prepared cRGD-linked PEG-b-poly(L-glutamic acid) (PEG-b-P(Glu)) micelles (cRGD/m) with different cRGD densities for delivery of (1,2-diaminocyclohexane) platinum(II) (DACHPt) to glioblastoma through the blood−brain tumor barrier (Figure 3).[87] Intravital confocal laser scanning microscopy revealed that compared with cyclic-Arg-Ala-Asp (cRAD)-linked counterparts (nontargeted control), cRGD/m with 20% cRGD accumulated rapidly and had high permeability from vessels into the tumor
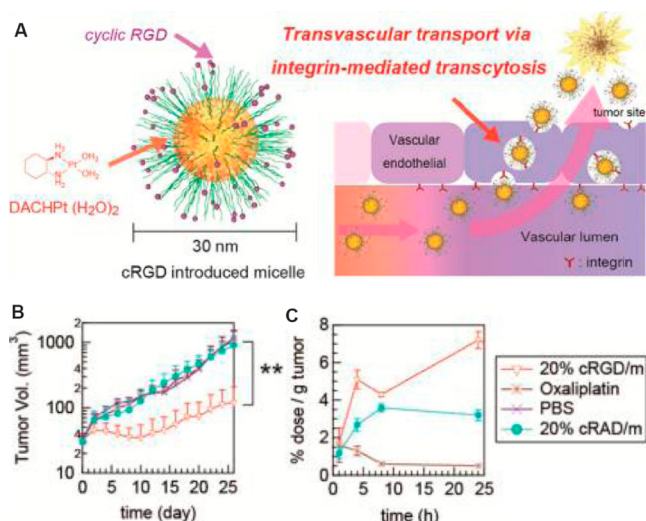
Figure 3. cRGD-conjugated PEG-*b*-P(Glu) micelles (cRGD/m) for targeted delivery of platinum anticancer drugs to glioblastoma through the BBB. (A) Schematic showing the structure of cRGD/m and transvascular transport of platinum via intergrin-mediated transcytosis; (B) tumor growth inhibition in mice bearing glioblastoma U87MG tumors following i.v. injection of cRGD/m, nontargeted micelles (cRAD/m), oxaliplatin, and PBS every other day (4 mg platinum/kg and 8 mg oxaliplatin/kg, three injections, *n* = 8); (C) platinum accumulation at tumors after i.v. injection with cRGD/m, cRAD/m, and oxaliplatin at different time points (*n* = 6). The data are shown as mean ± SD (**p < 0.01). Reproduced from ref 87. Copyright 2013 American Chemical Society.

parenchyma. In comparison with cRAD-linked micelles, cRGD/m showed selective and accelerated accumulation into tumors and produced significant antitumor effects in an orthotopic mouse model of U87MG human glioblastoma. Besides angiogenic endothelial cells and glioblastoma carcinoma, cRGD could also target to breast cancer, bladder cancer and prostate cancer. For example, Lavasanifar et al. demonstrated that cRGDfK decoration of PEO-*b*-PCL or PEO-*b*-poly(α-benzyl carboxylate-ε-caprolactone) (PEO-*b*-PBCL) nanoparticles enhanced the selective cytotoxicity of encapsulated PTX against MDA-MB-435 cells over normal HUVEC and MCF10A cells.[88] It is noted that p160 peptide decorated micelles showed better binding, internalization and specificity in MDA-MB-435 cells than cRGDfK-micelles. Duan et al. prepared cRGD-modified monomethoxy PEG-PLGA-poly(L-lysine) nanoparticles (MPEG-PLGA-PLL-cRGD NPs) with mitoxantrone (DHAQ, antitumor drug) or rhodamine B (Rb, fluorescence agent) loaded in their interior.[89] The in vitro and in vivo results showed that MPEG-PLGA-PLL-cRGD NPs were able to specifically target to MDA-MB-231 breast cancer cells and MDA-MB-231 breast cancer xenograft in mice, leading to significantly enhanced inhibition of tumor growth. Gan et al. reported that DOX-loaded cRGDfk-functionalized PEO-PCL micelles exhibited high affinity with T-24 bladder cancer cells and strong inhibitory effect on their proliferation.[90] Satchi-Fainaro et al. reported that PTX and cRGDfK$_2$ conjugated poly(glutamic acid) (PGA-PTX-E-(cRGDfK$_2$)) inhibited the growth of proliferating α$_v$β$_3$-expressing human umbilical vein endothelial cells (HUVEC), U87MG human glioblastoma, and 4T1 murine breast cancer.[91] Orthotopic studies in mice bearing murine 4T1 breast tumors demonstrated preferential accumulation of PGA-PTX-E-(cRGDfK$_2$) in

the tumor, leading to enhanced antitumor efficacy and a marked decrease in toxicity as compared with free PTX. Ghandehari et al. reported that *N*-(2-hydroxypropyl) methacrylamide (HPMA) copolymer-DTX-RGDfK conjugate with a hydrodynamic diameter of 3.0 nm demonstrated active binding to α$_v$β$_3$ integrins in both HUVEC and DU145 human prostate cancer cells and caused significant tumor regression compared to nontargeted HPMA-DTX counterparts in mice bearing DU145 human prostate tumor xenografts.[92]

The recently developed internalizing RGD (iRGD) can not only target to α$_v$β$_3$ integrin receptor, but also facilitate tumor penetration.[97,98] Jiang et al. prepared iRGD-decorated PTX-loaded micelles from PCL-*b*-poly(*N*-vinylpyrrolidone) (PCL-*b*-PVP) with different PVP block length.[93] The targeted micelles with a long PVP block exhibited long circulation time, high tumor accumulation and deep penetration, better tumor inhibition effect, and longer survival time as compared to Taxol in murine H22 hepatic tumor-bearing mice. In addition to cRGD and iRGD, several other peptides, such as octreotide, AP peptide, and tLyp-1 peptide, have been applied for targeted cancer chemotherapy. For example, Zhang et al. conjugated octreotide (Oct), an octapeptide analogue of endogenous somatostatin, onto the surface of PTX-loaded PEG-*b*-PCL micelles (Oct-M-PTX) for active targeting to MCF-7 breast cancer cells.[94] Oct-M-PTX was taken up by somatostatin receptors (SSTR) overexpressed MCF-7 cells via receptor-mediated endocytosis and exhibited increased cytotoxicity as compared to M-PTX (nontargeting control). AP peptide (CRKRLDRN) with specific binding affinity to IL-4 receptors of atherosclerotic plaques and breast tumor tissues was conjugated to DOX-loaded pH-sensitive micelles composed of PEG-PLA and MPEG-poly(β-amino ester) (PAE) block copolymers (DOX-AP-pH-PM).[95] The in vivo studies showed that DOX-AP-pH-PM resulted in 2-fold higher fluorescence intensity than nontargeted micelles in the MDA-MB231 tumor of mice and significantly more potent tumor inhibition than free DOX and DOX-pH-PMs. tLyp-1 peptide, a truncated form of LyP-1 with seven amino acids (CGNKRTR), contains both a tumor-homing motif targeted to the NRP receptor with high affinity and a cryptic CendR motif ((R/K)XX(R/K)), which is responsible for cell internalization and tissue penetration. The tLyp-1 peptide as a dual targeting ligand was conjugated to the surface of PTX-loaded PEG-PLA nanoparticles (tLyp-1-NP-PTX) via a maleimide−thiol coupling reaction.[96] Improved tumor accumulation and penetration of tLyp-1-NP was observed in both avascular C6 glioma spheroids and mice bearing intracranial C6 glioma. tLyp-1-NP-PTX treatment prolonged the survival of mice bearing intracranial C6 glioma as compared to nontargeting NP-PTX and Taxol (medium survival time: 37 d vs 28 and 23 d, respectively).

6. SACCHARIDE OR POLYSACCHARIDE-DIRECTED ACTIVE TARGETING POLYMERIC NANOPARTICLES

The cancerous cells often express different glycans as compared with the healthy ones, which renders saccharides an interesting ligand for tumor-specific drug delivery. In particular, hepatocellular carcinoma cells are known overexpressing the asialoglycoprotein receptors (ASGP-R).[99] In the past decade, saccharide (e.g., galactose and galactosamine) conjugated nanoparticles have been developed for targeted liver cancer therapy (Table 5). Various drug-loaded galactose-functionalized nanoparticles, such as DOX-loaded multifunctional micelles based on poly(*N*-isopropylacrylamide-*co*-methacryl acid)-*g*-PLA

Table 5. Saccharide or Polysaccharide-Directed Active Targeting Polymeric Nanoparticles for Cancer Treatment

construction	drug	target	ref
Gal-PEG-PLA/FITC-PEG-PLA/MPEG-PLA/P(NIPAAm-co-MAAc)-g-PLA micelles	DOX	hepatoma	100
Gal-CS-g-PNIPAm nanogels	ORI	hepatoma	101
Gal-PEG-PCL/PEG-SS-PCL micelles	DOX	hepatoma	102
Gal-HPMA-DOX prodrugs	DOX	hepatoma	103,104
Gal-PEG-PCL/PEG-PAC-PCL micelles	PTX	hepatoma	105
Gal-γ-PGA-PLA nanoparticles	PTX	hepatoma	106
HA-PTX micelles	PTX	colon cancer, breast cancer	109
HA-PEG-PLGA nanoparticles	DOX	Ehrlich ascites cancer	110
HA-PBLG polymersomes	DOX	breast cancer	111
HA-SS-DOCA micelles	PTX	breast cancer	112
HA-CA/PEG/APMA nanoparticles	PTX	squamous cell carcinoma	113

(P(NIPAAm-co-MAAc)-g-PLA)/MPEG-PLA/Gal-PEG-PLA)/fluorescein isothiocyanate (FITC)-PEG-PLA,[100] oridonin (ORI)-loaded galactosylated chitosan-g-PNIPAAm (Gal-CS-g-PNIPAAm) nanogels,[101] and DOX-loaded reduction-sensitive micelles based on PEG-SS-PCL/Gal-PEG-PCL,[102] were reported to possess high specificity and in vitro antitumor activity toward human hepatoma HepG2 cells. It should be noted that galactosamine-functionalized HPMA-DOX prodrugs (also known as PK2) represent an earliest example on active targeting nanomedicines.[103,104] The preclinical studies showed that i.v. administration of PK2 led to effective liver targeting with more than 70% of the dose of DOX being selectively

targeted to the liver in rats and mice. The clinical studies revealed approximately 30% of the drug delivered to the hepatic region at 24 h, as determined by planar whole body imaging, and a ratio of tumor tissue to normal liver uptake of approximately 1:3, as revealed by single photon emission computed tomography (SPECT) analysis. These clinical results confirmed that effective hepatic targeting can be achieved following an i.v. dose of 20 mg/m^2 DOX as PK2. We prepared galactose-decorated cross-linked biodegradable micelles from PEG-b-poly(acryloyl carbonate)-b-PCL and galactose-PEG-PCL copolymers (PEG-PAC-PCL/Gal-PEG-PCL) for hepatoma-targeted delivery of PTX.[105] The in vivo studies in human hepatoma (SMMC-7721)-bearing nude mice revealed that galactose-decorated PTX-loaded cross-linked PEG-PCL micelles inhibited the growth of the human hepatoma more effectively than PTX-loaded cross-linked micelles and galactose-decorated PTX-loaded non-cross-linked micelles. Sung et al. reported that PTX-loaded galactosamine-conjugated γ-PGA-PLA nanoparticles (Gal-P/NPs) had significantly higher antitumor activity than P/NPs in human hepatoma HepG2 cells.[106] The biodistribution and antitumor efficacy studies in hepatoma-tumor-bearing nude mice showed that a large number of the Gal-P/NPs were accumulated at the tumor site and compared with the groups injected with Phyxol (clinically available paclitaxel formulation) and P/NPs (non-targeting control), the group injected with the Gal-P/NPs revealed the highest efficacy in the tumor suppression.

In addition to saccharides, polysaccharides, in particular, HA, have received great interest for targeted drug delivery. HA as natural polymers have excellent biocompatibility and biodegradability.[107] Given the fact that HA binding receptors, such as CD44 and RHAMM, are overexpressed on the cell surface of several malignant tumors with high metastasis activity, HA has
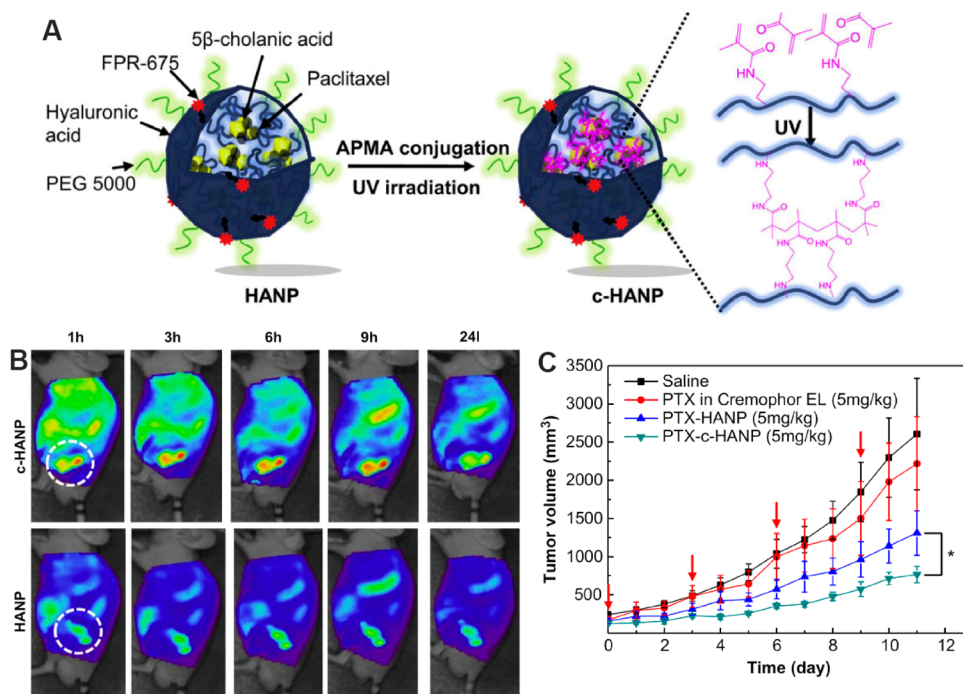

Figure 4. PEGylated photo-cross-linked HA-g-CA nanoparticles (c-HANPs) for PTX delivery and cancer chemotherapy. (A) Schematic illustration on preparation of c-HANPs by UV cross-linking; (B) whole body NIRF images of SCC7 tumor-bearing mice treated with FPR675-labeled HANP and c-HANP (white circles indicate tumor sites); (C) tumor growth of mice models treated with various PTX formulations (the red arrows indicate the time point for injection). The data are shown as mean ± SD (*p < 0.05). Reprinted with permission from ref 113. Copyright 2013 Elsevier.

been actively investigated for targeted delivery of various anticancer drugs.[108] Park et al. reported that HA-PTX conjugate micelles induced more pronounced cytotoxic effect to human colon cancer cell line (HCT-116) and breast cancer cell line (MCF-7) as compared to the conventional paclitaxel formulation.[109] Agrawal et al. reported that DOX-loaded HA-PEG-PLGA nanoparticles following 1 h i.v. injection into Ehrlich ascites tumor-bearing mice revealed 2-fold higher concentration of DOX in the tumor as compared to MPEG-PLGA nanoparticles.[110] The therapeutic efficacy studies showed that DOX-loaded HA-PEG-PLGA nanoparticles could effectively inhibit Ehrlich ascites tumor growth. Lecommandoux et al. developed DOX-loaded poly(γ-benzyl L-glutamate)-b-hyaluronan (PBLG-b-HA) polymersomes (PolyDOX).[111] The results suggested that intracellular delivery of PolyDOX was depended on the CD44 expression level in cells. The in vivo studies in breast tumor-bearing female Sprague–Dawley (SD) rats showed that PolyDOX significantly reduced tumor volume at 30 d treatment and in sharp contrast to free DOX treatment no mortality was observed after 60 d treatment with PolyDOX. Zhang et al. demonstrated that PTX-loaded redox-sensitive micelles based on HA-deoxycholic acid (HA-SS-DOCA) conjugates had increased antitumor activity of PTX against human breast MDA-MB-231 cells and significantly enhanced accumulation in the MDA-MB-231 tumor in mice.[112] Park et al. developed photo-cross-linked HA nanoparticles (c-HANPs) from PEG and acrylate-conjugated HA-5β-cholanic acid (HA-CA; Figure 4).[113] The in vivo studies in nude mice bearing squamous cell carcinoma (SCC7) revealed that PTX-loaded c-HANPs possessed high stability, enhanced tumor targeting ability (about 1.7-fold higher tumor accumulation than non-cross-linked HA-NPs), and superior therapeutic efficacy to the non-cross-linked counterparts and PTX in Cremophor EL. The ex vivo NIR imaging studies using Cy5.5-labeled HA-CA nanoparticles revealed strong fluorescence in the liver, which is possibly due to cellular uptake of the HA-CA nanoparticles by phagocytic cells of the reticuloendothelial system and by liver sinusoidal endothelial cells expressing the HA receptor CD44.[114]

7. SMALL MOLECULE-DIRECTED ACTIVE TARGETING POLYMERIC NANOPARTICLES

In the past decades, a variety of small molecules such as FA (vitamin B9), biotin (vitamin B7), glycyrrhizin, bisphosphonates, and ACUPA have been used as targeting ligands for cancer chemotherapy (Table 6). These small molecules are readily available, inexpensive, nontoxic, nonimmunogenic, and easy to modify and characterize.[115] FA is necessary for the synthesis of purines and pyrimidines. FA binds with a high affinity (in the nanomolar range) to the glycosylphosphatidylinositol-linked folate receptor, which is overexpressed in the cancerous cells as compared to the normal cells.[116] The expression levels of FA in tumors have been reported to be 100−300 times higher than in normal tissues.[117] FA-conjugated oil-encapsulating PEO-PPO-PEO/PEG shell cross-linked nanocapsules, which were prepared by dissolving an oil (Lipiodol) and an amine-reactive PEO-PPO-PEO derivative in dichloromethane and subsequently dispersing in an aqueous solution containing amine-functionalized six-arm-branched PEG by ultrasonication, for target-specific PTX delivery.[118] The targeted nanocapsules could effectively solubilize PTX in the inner lipiodol phase and significantly enhanced the cellular uptake and apoptotic effect of PTX against folate receptor

Table 6. Small Molecule Ligand-Directed Active Targeting Polymeric Nanoparticles for Cancer Treatment

construction	drug	target	ref
FA-PEG/PEO-PPO-PEO nanocapsules	PTX	epithelial cancer	[118]
FA-PEG-DSPE/MPEG-DSPE/DLPC stealth nanoparticles	DTX	breast cancer	[119]
FA-PEG-PLGA/MPEG-PLGA-DOX micelles	DOX	epithelial cancer	[120]
FA-PEG-PAsp(DIP)-CA micelles	PTX	hepatoma	[121]
FA-PEG-PCL-hyd-DOX micelles	DOX	epithelial cancer	[122]
biotin-PEG-PLA/PLGA nanoparticles	PTX	drug-resistant epithelial-like cancer	[124]
biotin-PEG-PLA/PLGA-PEI nanoparticles	PTX	drug-resistant epithelial-like cancer	[125]
ALG-GA nanoparticles	DOX	hepatoma	[126]
CMC-GL nanoparticles	PTX	hepatoma	[127]
Aln-PLGA/PVA nanoparticles	curcumin + bortezomib	bone metastasis	[128]
ACUPA-PEG-PLA/PEG-PLGA micelles	DTX	prostate cancer	[129]

overexpressing epithelial cancer cells (KB). Feng et al. designed and prepared a FA-conjugated nanoparticle of mixed lipid monolayer shell and biodegradable PLGA core for receptor-mediated delivery of DTX.[119] The mixed lipid monolayer shell includes three distinct functional components: 1,2-dilauroyl-phosphatidylocholine (DLPC), 1,2-distearoyl-sn-glycero-3-phosphoethanolamine-N-(MPEG-2000) (DSPE-PEG$_{2k}$), and 1,2-distearoyl-sn-glycero-3-phosphoethanolamine-N-(folate-PEG-5000 (DSPE-PEG$_{5k}$-FA), which facilitate quantitative control of the targeting effect by adjusting the lipid component ratio. DTX-loaded nanoparticles could target to human MCF-7 breast tumor and displayed 50.91 and 93.65% more effective than nontargeted formulation and Taxotere, respectively. Park et al. reported that folate-receptor targeted biodegradable polymeric micelles, self-assembled from DOX-PLGA-MPEG, PLGA-PEG-FA, and free base DOX, displayed increased DOX accumulation in the tumor tissue and significantly regressed tumor volume in human epidermal carcinoma (KB)-bearing nude mice.[120] Shuai et al. developed FA-conjugated, PTX and quantum dot (QD)-loaded, and pH-sensitive micelles based on PEG-poly(N-(N',N'-diisopropylaminoethyl) aspartamide)-CA (PEG-PAsp(DIP)-CA) for tumor-targeted intracellular drug release and fluorescent imaging (Figure 5).[121] The pH-sensitive PTX-loaded micelle exhibited the capability to turn drug release "off" at neutral pH, whereas it was "on" inside acidic lysosomes in vitro (with a drug release of 65 and 5% at pH 5.0 and 7.4, respectively). In nude mice bearing human hepatoma Bel-7402 tumor, tumor growth was completely stopped when the mice were treated with PTX-loaded targeted micelles. Zhou et al. reported that FA-functionalized DOX-conjugated micelles based on FA-PEG-PCL-hydrazone-DOX showed much better cellular uptake and higher cytotoxicity to human nasopharyngeal epidermoid carcinoma (KB) cells.[122] The in vivo studies in murine breast tumor-bearing mice indicated that targeted micelles enhanced accumulation of drug in the tumor sites and exhibited good antitumor efficacy. It should be noted, however, that excess FA would negatively affect the aqueous stability of nanoparticles leading to formation of insoluble aggregates.[123]

Biotin is a cell growth promoter. Biotin receptors are often overexpressed on the surface of rapidly proliferating cancer cells.[130] Panyam et al. designed and developed biotin-
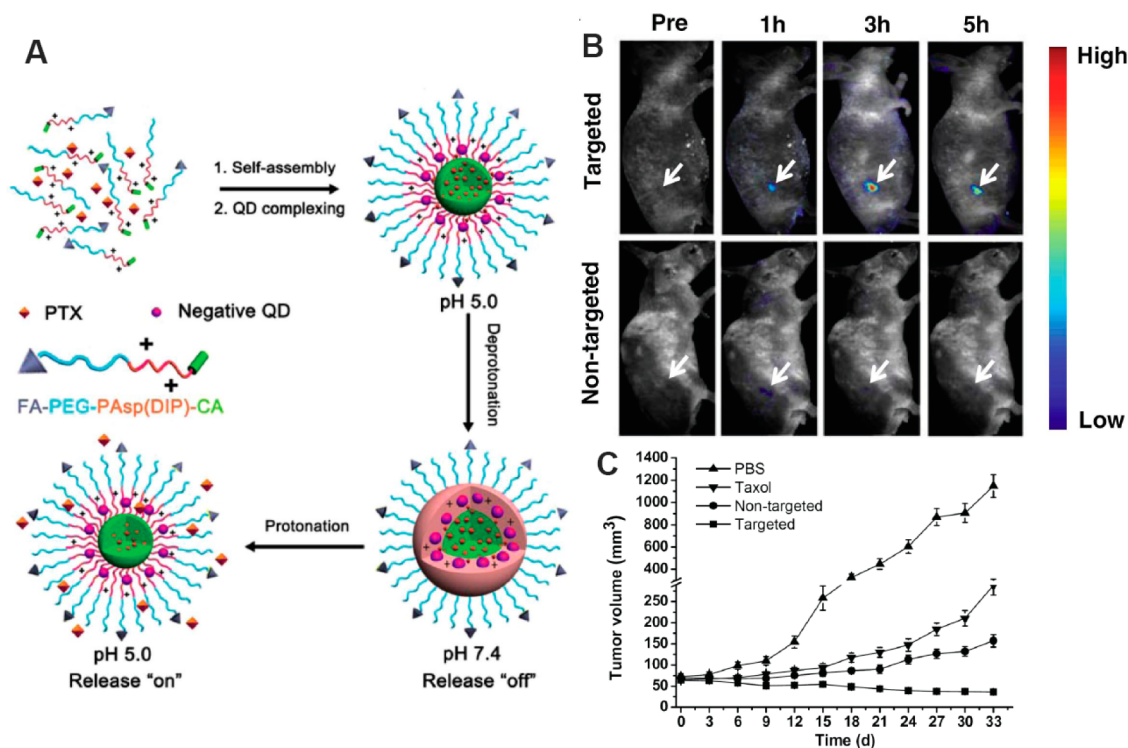
Figure 5. FA-directed multifunctional micelles for tumor-targeted pH-sensitive drug release and fluorescent imaging. (A) Illustrative preparation of PTX and QD-loaded micelle and pH-tunable drug release; (B) In vivo QD fluorescence images showing FA-enhanced tumor targeting of the QD-loaded targeted micelles after i.v. injection into nude mice bearing Bel-7402 subcutaneous xenograft (dose: 70 mg micelle/kg); and (C) tumor growth inhibition in nude mice bearing Bel-7402 tumor after i.v. injection of different formulations (dose: 1 mg PTX per kg body weight per injection for PTX-containing formulations; injection was performed at an interval of 3 days, n = 20). Reproduced from ref 121. Copyright 2012 Wiley-VCH Verlag GmbH & Co. KGaA, Weinheim. With permission from John Wiley and Sons.

functionalized PLGA/PLA-PEG nanoparticles for simultaneous and targeted delivery of PTX and tariquidar, a P-glycoprotein (P-gp) modulator, to overcome tumor drug resistance.[124] These dual agent targeting nanoparticles showed significantly higher cytotoxicity toward two drug-resistant cell lines, JC and NCI/ADR-RES, than nanoparticles loaded with PTX alone, due to increased PTX accumulation inside the drug-resistant tumor cells. The in vivo studies in a mouse model bearing drug-resistant epithelial-like cancer (JC) demonstrated that biotin-functionalized nanoparticles encapsulating both PTX and tariquidar caused significantly greater inhibition of tumor growth at a PTX dose that was ineffective in the absence of tariquidar. In a following study, to overcome tumor drug resistance, biotin-functionalized PLGA nanoparticles were developed from PLGA-polyethylenimine (PLGA-PEI) for targeted codelivery of P-gp targeted siRNA and PTX.[125] The in vivo studies in a mouse model of drug-resistant JC tumor demonstrated significantly greater inhibition of tumor growth following treatment with biotin-functionalized nanoparticles encapsulating both PTX and P-gp targeted siRNA, which could be correlated with effective silencing of the MDR1 gene that encodes for P-gp and with increased accumulation of PTX in drug-resistant tumor cells.

Glycyrrhetinic acid (GA) or glycyrrhizin (GL) is one of the main bioactive compounds extracted from licorice, which can be used to treat hepatitis and hepatotoxicity.[131] Due to their high binding ability to the cellular membrane of hepatocytes, GA or GL has been utilized as a specific ligand for hepatoma-targeting chemotherapy. Yuan et al. prepared DOX-loaded GA-modified alginate (ALG) nanoparticles (DOX/ALG-GA NPs)

for liver cancer therapy.[126] The biodistribution in Kuming mice showed that the concentration of DOX in the liver was 2.8- and 4.7-fold higher for DOX/ALG-GA NPs than for nontargeted counterpart and free DOX, respectively. DOX/GA-ALG NPs showed a tumor growth inhibition rate (IR) of 76.6% in mice bearing H22 liver tumors. Yin et al. found that glycyrrhizin-modified O-carboxymethyl chitosan nanoparticles (CMC-GL NPs) promoted liver cancer SMMC-7721 cell internalization by approximate 10-fold as compared to the nontargeted counterparts.[127] Compared with nontargeted formulations and free PTX, PTX-loaded CMCNP-GL NPs exhibited the highest antitumor activity in SMMC-7721 cells with an IC$_{50}$ of 2.7−3.2 μg/mL. In hepatic tumor bearing mice, PTX-loaded CMCNP-GL NPs showed an increased drug accumulation in tumor tissues and a remarkably enhanced antitumor efficacy with a tumor inhibition ratio of 87.5%, which was much higher than that of nontargeting formulation (64.0%) and PTX injection (34.5%).

Bisphosphonates, commonly used as palliative therapy, are bone seeking molecules which specially bind to active remodeling site of bone. The nitrogen containing bisphosphonates, such as alendronate (Aln), is very efficient in binding to the bone and reducing bone resorption.[132] Vishwanatha et al. prepared Aln conjugated PLGA/PVA nanoparticles (Aln-PLGA/PVA NPs) to coencapsulate curcumin and bortezomib for targeted treatment of bone metastasis cancer.[128] The in vivo studies in an intraosseous model of bone metastasis showed that Aln-PLGA/PVA NPs resulted in a high localization to the bone and a significant deduction of tumor growth rate along with protection of bone resorption.

ACUPA can selectively bind to PSMA that is overexpressed on prostate cancer cells and on the neovasculature of most nonprostate solid tumors. Langer et al. reported design, development and clinical translation of a targeted polymeric nanoparticle (TNP) containing DTX and ACUPA ligands for the treatment of patients with solid tumors.[129] DTX-TNP (BIND-014) was prepared with different physiochemical properties (e.g., particle sizes and targeting ligand densities). DTX-TNPs had a blood circulation half-life of about 20 h and minimal liver accumulation. In tumor-bearing mice, rats, and nonhuman primates, DTX-TNP displayed prolonged circulation in the vascular compartment with total DTX plasma concentrations remaining at least 100-fold higher than a solvent-based DTX formulation (sb-DTX) for more than 24 h. The initial clinical studies in patients with advanced solid tumors revealed that DTX-TNP gave a pharmacological profile differentiated from sb-DTXL, including pharmacokinetics consistent with preclinical data and cases of tumor shrinkage at doses below the sb-DTX dose typically used in the clinic.

8. CONCLUSIONS AND PERSPECTIVES

In the past decade, we have witnessed a rapid development of ligand-directed active tumor targeting polymeric nanoparticles for cancer chemotherapy. The in vivo studies in different tumor models have demonstrated that ligand-installed polymeric nanoparticles can enhance retention and accumulation of drugs in the tumor tissue, facilitate targeted cell uptake, increase therapeutic efficacy, and decrease systemic side effects. Notably, two active targeting polymeric nanoparticulate formulations (PK2 and BIND-014) have been translated to the clinical evaluation of patients with liver and prostate tumors, respectively. We anticipate that, in the next 10 years, a growing number of active targeting nanoparticulate drugs will enter the different phases of clinical trials worldwide for the treatment of various malignant tumors that currently can not properly be treated.

It should be noted, however, that though the concept of active tumor targeting has been proposed for about two decades, there is a scarcity of systemic preclinical and translational research of ligand-directed polymeric nanoparticulate drug delivery systems for targeted cancer chemotherapy. It is not uncommon that in vivo therapeutic experiments are carried out with very few active targeting nanoscale drug formulations, partly due to the high cost and stringent governmental regulations on experimental animals. Moreover, there is absence of standardized in vivo tests and the experimental set-ups typically vary from one to another, which render it essentially impossible to compare results from different research groups. In the past, most preclinical studies are performed using nude mice bearing subcutaneous tumor xenografts, which are questionable models as they possess characteristics differentiated from human cancers. It should further be noted that occurrence of drug resistance,[133,134] tumor metastasis,[135,136] and presence of cancer stem cells[137,138] are the major obstacles for effective cancer chemotherapy. In spite of their significance, there are few studies on the development of polymeric nanoparticles recognizing and targeting to metastatic cancer cells and cancer stem cells. In order to achieve more accurate assessment on the therapeutic performance of active targeting drug formulations, in situ cancer models, drug-resistant cancer models, metastatic cancer models, and circulating cancer stem cell models should be established and applied for future in vivo experiments. In terms

of vehicles, efforts should be directed to the design and development of innovative and smart targeting systems that can not only preferentially accumulate at the tumor site resulting in effective eradication of solid tumor(s) but also selectively recognize and kill circulating metastatic tumor cells, drug-resistant tumor cells as well as multidrug resistant cancer stem cells. The next generation of ligand-directed active targeting polymeric nanoparticles should ideally meet following requirements: (i) they have a high drug loading capacity; (ii) they are robust in the bloodstream with minimal premature drug release; (iii) they are specifically recognized and internalized by target cells including solid tumor cells, metastatic tumor cells, drug-resistant tumor cells and cancer stem cells; and (iv) they can efficiently release therapeutics at the site of action via either an internal or external stimulus. We are convinced that with rationale design, systemic investigation, and close collaboration with medical doctors and pharmaceutical industry, ligand-directed active tumor targeting polymeric nanoparticulate anticancer drugs will soon be translated to the clinics: safe and efficient targeted cancer chemotherapy modality is not a dream.

■ AUTHOR INFORMATION

Corresponding Authors
*E-mail: cdeng@suda.edu.cn.
*E-mail: zyzhong@suda.edu.cn.

Notes
The authors declare no competing financial interest.

■ REFERENCES

(1) Chabner, B. A.; Roberts, T. G. *Nat. Rev. Cancer* **2005**, *5*, 65−72.
(2) Cairns, R.; Papandreou, I.; Denko, N. *Mol. Cancer Res.* **2006**, *4*, 61−70.
(3) Zitvogel, L.; Kepp, O.; Kroemer, G. *Nat. Rev. Clin. Oncol.* **2011**, *8*, 151−160.
(4) Clevers, H. *Nat. Med.* **2011**, 313−319.
(5) Brigger, I.; Dubernet, C.; Couvreur, P. *Adv. Drug Delivery Rev.* **2012**, *64*, 24−36.
(6) Peer, D.; Karp, J. M.; Hong, S.; Farokhzad, O. C.; Margalit, R.; Langer, R. *Nat. Nanotechnol.* **2007**, *2*, 751−760.
(7) Wang, A. Z.; Langer, R.; Farokhzad, O. C. *Annu. Rev. Med.* **2012**, *63*, 185−198.
(8) Davis, M. E.; Chen, Z.; Shin, D. M. *Nat. Rev. Drug Discovery* **2008**, *7*, 771−782.
(9) Elsabahy, M.; Wooley, K. L. *Chem. Soc. Rev.* **2012**, *41*, 2545−2561.
(10) Wiradharma, N.; Zhang, Y.; Venkataraman, S.; Hedrick, J. L.; Yang, Y. Y. *Nano Today* **2009**, *4*, 302−317.
(11) Brannon-Peppas, L.; Blanchette, J. O. *Adv. Drug Delivery Rev.* **2012**, *64*, 206−212.
(12) Fang, J.; Nakamura, H.; Maeda, H. *Adv. Drug Delivery Rev.* **2011**, *63*, 136−151.
(13) Kim, T.-Y.; Kim, D.-W.; Chung, J.-Y.; Shin, S. G.; Kim, S.-C.; Heo, D. S.; Kim, N. K.; Bang, Y.-J. *Clin. Cancer Res.* **2004**, *10*, 3708−3716.

(14) Matsumura, Y.; Hamaguchi, T.; Ura, T.; Muro, K.; Yamada, Y.; Shimada, Y.; Shirao, K.; Okusaka, T.; Ueno, H.; Ikeda, M. *Br. J. Cancer* **2004**, *91*, 1775−1781.

(15) Hamaguchi, T.; Matsumura, Y.; Suzuki, M.; Shimizu, K.; Goda, R.; Nakamura, I.; Nakatomi, I.; Yokoyama, M.; Kataoka, K.; Kakizoe, T. *Br. J. Cancer* **2005**, *92*, 1240−1246.

(16) Plummer, R.; Wilson, R.; Calvert, H.; Boddy, A.; Griffin, M.; Sludden, J.; Tilby, M.; Eatock, M.; Pearson, D.; Ottley, C. *Br. J. Cancer* **2011**, *104*, 593−598.

(17) Petros, R. A.; DeSimone, J. M. *Nat. Rev. Drug Discovery* **2010**, *9*, 615−627.

(18) Allen, T. M. *Nat. Rev. Cancer* **2002**, *2*, 750−763.

(19) Koo, H.; Huh, M. S.; Sun, I.-C.; Yuk, S. H.; Choi, K.; Kim, K.; Kwon, I. C. *Acc. Chem. Res.* **2011**, *44*, 1018−1028.

(20) Nicolas, J.; Mura, S.; Brambilla, D.; Mackiewicz, N.; Couvreur, P. *Chem. Soc. Rev.* **2013**, *42*, 1147−1235.

(21) Byrne, J. D.; Betancourt, T.; Brannon-Peppas, L. *Adv. Drug Delivery Rev.* **2008**, *60*, 1615−1626.

(22) Kamaly, N.; Xiao, Z.; Valencia, P. M.; Radovic-Moreno, A. F.; Farokhzad, O. C. *Chem. Soc. Rev.* **2012**, *41*, 2971−3010.

(23) Marcucci, F.; Lefoulon, F. *Drug Discovery Today* **2004**, *9*, 219−228.

(24) Danhier, F.; Feron, O.; Préat, V. *J. Controlled Release* **2010**, *148*, 135−146.

(25) Soppimath, K. S.; Aminabhavi, T. M.; Kulkarni, A. R.; Rudzinski, W. E. *J. Controlled Release* **2001**, *70*, 1−20.

(26) Duncan, R. *Nat. Rev. Cancer* **2006**, *6*, 688−701.

(27) Li, C.; Wallace, S. *Adv. Drug Delivery Rev.* **2008**, *60*, 886−898.

(28) Pasut, G.; Veronese, F. M. *Prog. Polym. Sci.* **2007**, *32*, 933−961.

(29) Amoozgar, Z.; Yeo, Y. *Nanomed. Nanobiotechnol.* **2012**, *4*, 219−233.

(30) Hu, C.-M. J.; Fang, R. H.; Luk, B. T.; Zhang, L. *Nanoscale* **2014**, *6*, 65−75.

(31) Kataoka, K.; Harada, A.; Nagasaki, Y. *Adv. Drug Delivery Rev.* **2012**, *64*, 37−48.

(32) Matsumura, Y.; Kataoka, K. *Cancer Sci.* **2009**, *100*, 572−579.

(33) Deng, C.; Jiang, Y.; Cheng, R.; Meng, F.; Zhong, Z. *Nano Today* **2012**, *7*, 467−480.

(34) Bae, Y. H.; Yin, H. *J. Controlled Release* **2008**, *131*, 2−4.

(35) Kabanov, A. V.; Vinogradov, S. V. *Angew. Chem., Int. Ed.* **2009**, *48*, 5418−5429.

(36) Chacko, R. T.; Ventura, J.; Zhuang, J.; Thayumanavan, S. *Adv. Drug Delivery Rev.* **2012**, *64*, 836−851.

(37) Oh, J. K.; Drumright, R.; Siegwart, D. J.; Matyjaszewski, K. *Prog. Polym. Sci.* **2008**, *33*, 448−477.

(38) Mora-Huertas, C.; Fessi, H.; Elaissari, A. *Int. J. Pharm.* **2010**, *385*, 113−142.

(39) Meier, W. *Chem. Soc. Rev.* **2000**, *29*, 295−303.

(40) Ortiz, V.; Nielsen, S. O.; Discher, D. E.; Klein, M. L.; Lipowsky, R.; Shillcock, J. *J. Phys. Chem. B* **2005**, *109*, 17708−17714.

(41) Meng, F.; Zhong, Z.; Feijen, J. *Biomacromolecules* **2009**, *10*, 197−209.

(42) Gu, F. X.; Karnik, R.; Wang, A. Z.; Alexis, F.; Levy-Nissenbaum, E.; Hong, S.; Langer, R. S.; Farokhzad, O. C. *Nano Today* **2007**, *2*, 14−21.

(43) Gratton, S. E.; Ropp, P. A.; Pohlhaus, P. D.; Luft, J. C.; Madden, V. J.; Napier, M. E.; DeSimone, J. M. *Proc. Natl. Acad. Sci. U.S.A.* **2008**, *105*, 11613−11618.

(44) Decuzzi, P.; Godin, B.; Tanaka, T.; Lee, S.-Y.; Chiappini, C.; Liu, X.; Ferrari, M. *J. Controlled Release* **2010**, *141*, 320−327.

(45) O'Reilly, R. K.; Hawker, C. J.; Wooley, K. L. *Chem. Soc. Rev.* **2006**, *35*, 1068−1083.

(46) Owen, S. C.; Chan, D. P.; Shoichet, M. S. *Nano Today* **2012**, *7*, 53−65.

(47) Adams, G. P.; Schier, R.; McCall, A. M.; Simmons, H. H.; Horak, E. M.; Alpaugh, R. K.; Marks, J. D.; Weiner, L. M. *Cancer Res.* **2001**, *61*, 4750−4755.

(48) Schrama, D.; Reisfeld, R. A.; Becker, J. C. *Nat. Rev. Drug Discovery* **2006**, *5*, 147−159.

(49) Acharya, S.; Dilnawaz, F.; Sahoo, S. K. *Biomaterials* **2009**, *30*, 5737−5750.

(50) Peng, X.-H.; Wang, Y.; Huang, D.; Wang, Y.; Shin, H. J.; Chen, Z.; Spewak, M. B.; Mao, H.; Wang, X.; Wang, Y. *ACS Nano* **2011**, *5*, 9480−9493.

(51) Lee, H.; Hu, M.; Reilly, R. M.; Allen, C. *Mol. Pharmaceutics* **2007**, *4*, 769−781.

(52) Lee, H.; Fonge, H.; Hoang, B.; Reilly, R. M.; Allen, C. *Mol. Pharmaceutics* **2010**, *7*, 1195−1208.

(53) Tseng, C.-L.; Su, W.-Y.; Yen, K.-C.; Yang, K.-C.; Lin, F.-H. *Biomaterials* **2009**, *30*, 3476−3485.

(54) Sandoval, M. A.; Sloat, B. R.; Lansakara-P, D. S.; Kumar, A.; Rodriguez, B. L.; Kiguchi, K.; DiGiovanni, J.; Cui, Z. *J. Controlled Release* **2012**, *157*, 287−296.

(55) Shi, M.; Ho, K.; Keating, A.; Shoichet, M. S. *Adv. Funct. Mater.* **2009**, *19*, 1689−1696.

(56) Liu, Y.; Li, K.; Liu, B.; Feng, S.-S. *Biomaterials* **2010**, *31*, 9145−9155.

(57) Zhao, J.; Mi, Y.; Liu, Y.; Feng, S.-S. *Biomaterials* **2012**, *33*, 1948−1958.

(58) Debotton, N.; Parnes, M.; Kadouche, J.; Benita, S. *J. Controlled Release* **2008**, *127*, 219−230.

(59) Jin, C.; Qian, N.; Zhao, W.; Yang, W.; Bai, L.; Wu, H.; Wang, M.; Song, W.; Dou, K. *Biomacromolecules* **2010**, *11*, 2422−2431.

(60) Song, H.; He, R.; Wang, K.; Ruan, J.; Bao, C.; Li, N.; Ji, J.; Cui, D. *Biomaterials* **2010**, *31*, 2302−2312.

(61) Xu, Q.; Liu, Y.; Su, S.; Li, W.; Chen, C.; Wu, Y. *Biomaterials* **2012**, *33*, 1627−1639.

(62) Hong, M.; Zhu, S.; Jiang, Y.; Tang, G.; Pei, Y. *J. Controlled Release* **2009**, *133*, 96−102.

(63) Hong, M.; Zhu, S.; Jiang, Y.; Tang, G.; Sun, C.; Fang, C.; Shi, B.; Pei, Y. *J. Controlled Release* **2010**, *141*, 22−29.

(64) Gan, C. W.; Feng, S.-S. *Biomaterials* **2010**, *31*, 7748−7757.

(65) Pang, Z.; Gao, H.; Yu, Y.; Guo, L.; Chen, J.; Pan, S.; Ren, J.; Wen, Z.; Jiang, X. *Bioconjugate Chem.* **2011**, *22*, 1171−1180.

(66) Pang, Z.; Feng, L.; Hua, R.; Chen, J.; Gao, H.; Pan, S.; Jiang, X.; Zhang, P. *Mol. Pharmaceutics* **2010**, *7*, 1995−2005.

(67) Tai, W.; Mahato, R.; Cheng, K. *J. Controlled Release* **2010**, *146*, 264−275.

(68) Manjappa, A. S.; Chaudhari, K. R.; Venkataraju, M. P.; Dantuluri, P.; Nanda, B.; Sidda, C.; Sawant, K. K.; Ramachandra Murthy, R. S. *J. Controlled Release* **2011**, *150*, 2−22.

(69) Qian, Z. M.; Li, H.; Sun, H.; Ho, K. *Pharmacol. Rev.* **2002**, *54*, 561−587.

(70) González-Chávez, S. A.; Arévalo-Gallegos, S.; Rascón-Cruz, Q. *Int. J. Antimicrob. Agents* **2009**, *33* (301), e1−301−e8.

(71) Lee, J. H.; Yigit, M. V.; Mazumdar, D.; Lu, Y. *Adv. Drug Delivery Rev.* **2010**, *62*, 592−605.

(72) Xiao, Z.; Farokhzad, O. C. *ACS Nano* **2012**, *6*, 3670−3676.

(73) Gu, F.; Zhang, L.; Teply, B. A.; Mann, N.; Wang, A.; Radovic-Moreno, A. F.; Langer, R.; Farokhzad, O. C. *Proc. Natl. Acad. Sci. U.S.A.* **2008**, *105*, 2586−2591.

(74) Kolishetti, N.; Dhar, S.; Valencia, P. M.; Lin, L. Q.; Karnik, R.; Lippard, S. J.; Langer, R.; Farokhzad, O. C. *Proc. Natl. Acad. Sci. U.S.A.* **2010**, *107*, 17939−17944.

(75) Xu, W.; Siddiqui, I. A.; Nihal, M.; Pilla, S.; Rosenthal, K.; Mukhtar, H.; Gong, S. *Biomaterials* **2013**, *34*, 5244−5253.

(76) Gao, H.; Qian, J.; Yang, Z.; Pang, Z.; Xi, Z.; Cao, S.; Wang, Y.; Pan, S.; Zhang, S.; Wang, W. *Biomaterials* **2012**, *33*, 6264−6272.

(77) Guo, J.; Gao, X.; Su, L.; Xia, H.; Gu, G.; Pang, Z.; Jiang, X.; Yao, L.; Chen, J.; Chen, H. *Biomaterials* **2011**, *32*, 8010−8020.

(78) Gao, H.; Qian, J.; Cao, S.; Yang, Z.; Pang, Z.; Pan, S.; Fan, L.; Xi, Z.; Jiang, X.; Zhang, Q. *Biomaterials* **2012**, *33*, 5115−5123.

(79) Li, X.; Zhao, Q.; Qiu, L. *J. Controlled Release* **2013**, *171*, 152−162.

(80) Ruoslahti, E. *Adv. Mater.* **2012**, *24*, 3747−3756.

(81) Desgrosellier, J. S.; Cheresh, D. A. *Nat. Rev. Cancer* **2010**, *10*, 9−22.

(82) Nasongkla, N.; Shuai, X.; Ai, H.; Weinberg, B. D.; Pink, J.; Boothman, D. A.; Gao, J. *Angew. Chem., Int. Ed.* **2004**, *116*, 6483–6487.

(83) Nasongkla, N.; Bey, E.; Ren, J.; Ai, H.; Khemtong, C.; Guthi, J. S.; Chin, S.-F.; Sherry, A. D.; Boothman, D. A.; Gao, J. *Nano Lett.* **2006**, *6*, 2427–2430.

(84) Graf, N.; Bielenberg, D. R.; Kolishetti, N.; Muus, C.; Banyard, J.; Farokhzad, O. C.; Lippard, S. J. *ACS Nano* **2012**, *6*, 4530–4539.

(85) Zhan, C.; Gu, B.; Xie, C.; Li, J.; Liu, Y.; Lu, W. *J. Controlled Release* **2010**, *143*, 136–142.

(86) Jiang, X.; Sha, X.; Xin, H.; Chen, L.; Gao, X.; Wang, X.; Law, K.; Gu, J.; Chen, Y.; Jiang, Y. *Biomaterials* **2011**, *32*, 9457–9469.

(87) Miura, Y.; Takenaka, T.; Toh, K.; Wu, S.; Nishihara, H.; Kano, M. R.; Ino, Y.; Nomoto, T.; Matsumoto, Y.; Koyama, H.; Cabral, H.; Nishiyama, N.; Kataoka, K. *ACS Nano* **2013**, *7*, 8583–8592.

(88) Shahin, M.; Ahmed, S.; Kaur, K.; Lavasanifar, A. *Biomaterials* **2011**, *32*, 5123–5133.

(89) Liu, P.; Qin, L.; Wang, Q.; Sun, Y.; Zhu, M.; Shen, M.; Duan, Y. *Biomaterials* **2012**, *33*, 6739–6747.

(90) Zhou, D.; Zhang, G.; Gan, Z. *J. Controlled Release* **2013**, *169*, 204–210.

(91) Eldar-Boock, A.; Miller, K.; Sanchis, J.; Lupu, R.; Vicent, M. J.; Satchi-Fainaro, R. *Biomaterials* **2011**, *32*, 3862–3874.

(92) Ray, A.; Larson, N.; Pike, D. B.; Grüner, M.; Naik, S.; Bauer, H.; Malugin, A.; Greish, K.; Ghandehari, H. *Mol. Pharmaceutics* **2011**, *8*, 1090–1099.

(93) Zhu, Z.; Xie, C.; Liu, Q.; Zhen, X.; Zheng, X.; Wu, W.; Li, R.; Ding, Y.; Jiang, X.; Liu, B. *Biomaterials* **2011**, *32*, 9525–9535.

(94) Zhang, Y.; Zhang, H.; Wang, X.; Wang, J.; Zhang, X.; Zhang, Q. *Biomaterials* **2012**, *33*, 679–691.

(95) Wu, X. L.; Kim, J. H.; Koo, H.; Bae, S. M.; Shin, H.; Kim, M. S.; Lee, B.-H.; Park, R.-W.; Kim, I.-S.; Choi, K. *Bioconjugate Chem.* **2010**, *21*, 208–213.

(96) Hu, Q.; Gao, X.; Gu, G.; Kang, T.; Tu, Y.; Liu, Z.; Song, Q.; Yao, L.; Pang, Z.; Jiang, X. *Biomaterials* **2013**, *34*, 5640–5650.

(97) Sugahara, K. N.; Teesalu, T.; Karmali, P. P.; Kotamraju, V. R.; Agemy, L.; Girard, O. M.; Hanahan, D.; Mattrey, R. F.; Ruoslahti, E. *Cancer Cell* **2009**, *16*, 510–520.

(98) Agemy, L.; Friedmann-Morvinski, D.; Kotamraju, V. R.; Roth, L.; Sugahara, K. N.; Girard, O. M.; Mattrey, R. F.; Verma, I. M.; Ruoslahti, E. *Proc. Natl. Acad. Sci. U.S.A.* **2011**, *108*, 17450–17455.

(99) Lemarchand, C.; Gref, R.; Couvreur, P. *Eur. J. Pharm. Biopharm.* **2004**, *58*, 327–341.

(100) Huang, C. K.; Lo, C. L.; Chen, H. H.; Hsiue, G. H. *Adv. Funct. Mater.* **2007**, *17*, 2291–2297.

(101) Duan, C.; Gao, J.; Zhang, D.; Jia, L.; Liu, Y.; Zheng, D.; Liu, G.; Tian, X.; Wang, F.; Zhang, Q. *Biomacromolecules* **2011**, *12*, 4335–4343.

(102) Zhong, Y.; Yang, W.; Sun, H.; Cheng, R.; Meng, F.; Deng, C.; Zhong, Z. *Biomacromolecules* **2013**, *14*, 3723–3730.

(103) Duncan, R.; Seymour, L.; O'Hare, K.; Flanagan, P.; Wedge, S.; Hume, I.; Ulbrich, K.; Strohalm, J.; Subr, V.; Spreafico, F. *J. Controlled Release* **1992**, *19*, 331–346.

(104) Julyan, P. J.; Seymour, L. W.; Ferry, D. R.; Daryani, S.; Boivin, C. M.; Doran, J.; David, M.; Anderson, D.; Christodoulou, C.; Young, A. M. *J. Controlled Release* **1999**, *57*, 281–290.

(105) Yang, R.; Meng, F.; Ma, S.; Huang, F.; Liu, H.; Zhong, Z. *Biomacromolecules* **2011**, *12*, 3047–3055.

(106) Liang, H.-F.; Chen, C.-T.; Chen, S.-C.; Kulkarni, A. R.; Chiu, Y.-L.; Chen, M.-C.; Sung, H.-W. *Biomaterials* **2006**, *27*, 2051–2059.

(107) Mizrahy, S.; Peer, D. *Chem. Soc. Rev.* **2012**, *41*, 2623–2640.

(108) Oh, E. J.; Park, K.; Kim, K. S.; Kim, J.; Yang, J.-A.; Kong, J.-H.; Lee, M. Y.; Hoffman, A. S.; Hahn, S. K. *J. Controlled Release* **2010**, *141*, 2–12.

(109) Lee, H.; Lee, K.; Park, T. G. *Bioconjugate Chem.* **2008**, *19*, 1319–1325.

(110) Yadav, A. K.; Mishra, P.; Mishra, A. K.; Mishra, P.; Jain, S.; Agrawal, G. P. *Nanomedicine* **2007**, *3*, 246–257.

(111) Upadhyay, K. K.; Bhatt, A. N.; Mishra, A. K.; Dwarakanath, B. S.; Jain, S.; Schatz, C.; Le Meins, J.-F.; Farooque, A.; Chandraiah, G.; Jain, A. K. *Biomaterials* **2010**, *31*, 2882–2892.

(112) Li, J.; Huo, M.; Wang, J.; Zhou, J.; Mohammad, J. M.; Zhang, Y.; Zhu, Q.; Waddad, A. Y.; Zhang, Q. *Biomaterials* **2012**, *33*, 2310–2320.

(113) Yoon, H. Y.; Koo, H.; Choi, K. Y.; Chan Kwon, I.; Choi, K.; Park, J. H.; Kim, K. *Biomaterials* **2013**, *34*, 5273–5280.

(114) Choi, K. Y.; Chung, H.; Min, K. H.; Yoon, H. Y.; Kim, K.; Park, J. H.; Kwon, I. C.; Jeong, S. Y. *Biomaterials* **2010**, *31*, 106–114.

(115) Drabovich, A. P.; Berezovski, M. V.; Musheev, M. U.; Krylov, S. N. *Anal. Chem.* **2008**, *81*, 490–494.

(116) Lu, Y.; Low, P. S. *Adv. Drug Delivery Rev.* **2012**, *64*, 342–352.

(117) Low, P. S.; Henne, W. A.; Doorneweerd, D. D. *Acc. Chem. Res.* **2007**, *41*, 120–129.

(118) Bae, K. H.; Lee, Y.; Park, T. G. *Biomacromolecules* **2007**, *8*, 650–656.

(119) Liu, Y.; Li, K.; Pan, J.; Liu, B.; Feng, S.-S. *Biomaterials* **2010**, *31*, 330–338.

(120) Yoo, H. S.; Park, T. G. *J. Controlled Release* **2004**, *96*, 273–283.

(121) Wang, W.; Cheng, D.; Gong, F.; Miao, X.; Shuai, X. *Adv. Mater.* **2012**, *24*, 115–120.

(122) Guo, X.; Shi, C.; Wang, J.; Di, S.; Zhou, S. *Biomaterials* **2013**, *34*, 4544–4554.

(123) Cao, W.; Zhou, J.; Mann, A.; Wang, Y.; Zhu, L. *Biomacromolecules* **2011**, *12*, 2697–2707.

(124) Patil, Y.; Sadhukha, T.; Ma, L.; Panyam, J. *J. Controlled Release* **2009**, *136*, 21–29.

(125) Patil, Y. B.; Swaminathan, S. K.; Sadhukha, T.; Ma, L.; Panyam, J. *Biomaterials* **2010**, *31*, 358–365.

(126) Zhang, C.; Wang, W.; Liu, T.; Wu, Y.; Guo, H.; Wang, P.; Tian, Q.; Wang, Y.; Yuan, Z. *Biomaterials* **2012**, *33*, 2187–2196.

(127) Shi, L.; Tang, C.; Yin, C. *Biomaterials* **2012**, *33*, 7594–7604.

(128) Thamake, S. I.; Raut, S. L.; Gryczynski, Z.; Ranjan, A. P.; Vishwanatha, J. K. *Biomaterials* **2012**, *33*, 7164–7173.

(129) Hrkach, J.; Von Hoff, D.; Ali, M. M.; Andrianova, E.; Auer, J.; Campbell, T.; De Witt, D.; Figa, M.; Figueiredo, M.; Horhota, A. *Sci. Transl. Med.* **2012**, *4*, 128ra39–128ra39.

(130) Russell-Jones, G.; McTavish, K.; McEwan, J.; Rice, J.; Nowotnik, D. *J. Inorg. Biochem.* **2004**, *98*, 1625–1633.

(131) Negishi, M.; Irie, A.; Nagata, N.; Ichikawa, A. *Biochim. Biophys. Acta* **1991**, *1066*, 77–82.

(132) Giger, E. V.; Castagner, B.; Leroux, J.-C. *J. Controlled Release* **2013**, *167*, 175–188.

(133) Gottesman, M. M. *Annu. Rev. Med.* **2002**, *53*, 615–627.

(134) Szakács, G.; Paterson, J. K.; Ludwig, J. A.; Booth-Genthe, C.; Gottesman, M. M. *Nat. Rev. Drug Discovery* **2006**, *5*, 219–234.

(135) Zetter, P.; Bruce, R. *Annu. Rev. Med.* **1998**, *49*, 407–424.

(136) Chambers, A. F.; Groom, A. C.; MacDonald, I. C. *Nat. Rev. Cancer* **2002**, *2*, 563–572.

(137) Visvader, J. E.; Lindeman, G. J. *Nat. Rev. Cancer* **2008**, *8*, 755–768.

(138) Dean, M.; Fojo, T.; Bates, S. *Nat. Rev. Cancer* **2005**, *5*, 275–284.